Journal of Archaeological Science: Reports 45 (2022) 103627

Contents lists available at ScienceDirect

Journal of Archaeological Science: Reports

journal homepage: www.elsevier.com/locate/jasrep

The production of western Greek amphorae in Agrigento (Southern Sicily): An archaeometric and archaeological characterisation of the late 6th-4th centuries BCE series

G. Montana [a,1], L. Randazzo [a,1], M. Gasparo Morticelli [a], V. Baldoni [b], B. Bechtold [c,*]

[a] Dipartimento di Scienze della Terra e del Mare (DiSTeM), Università degli Studi Palermo, Italy
[b] Dipartimento di Storia Culture Civiltà (DiSCi), Università di Bologna, Italy
[c] Institut für Klassische Archäologie, Universität Wien, Austria

ARTICLE INFO

Keywords:
Sicily
Agrigento
Western Greek amphorae
Local production
Kiln area
Petrography
Chemical analyses

ABSTRACT

This paper aims at an interdisciplinary, archaeological and archaeometric characterisation of the western Greek amphorae series produced in late Archaic and Classical-period Agrigento (southern Sicily). The research is based on a macroscopic examination, according to the standardised methods of Fabrics of the Central Mediterranean (FACEM), combined with petrographic analyses of 21 amphorae samples of presumed local fabric found in Agrigento itself. These were found in the artisanal area outside *Porta V*, in the excavations South of the temple of Zeus, and in several Sicilian consumption sites. Furthermore, a selection of 12 coarse ware samples and three tiles, all of supposed local manufacture and unearthed in Agrigento, has been investigated. For comparison, 12 raw clays sampled in the gullies between the *Tempio di Giunone* and the *Tempio della Concordia* have been included in this study and are complimented by chemical analyses (ICP-MS and ICP/OES) undertaken on a group of 19 ceramic samples and seven raw materials. As a result, our study confirms the local manufacture of the entire selection of 36 ceramic samples and the more than acceptable petrographic and chemical homogeneity of the ceramic pastes produced with locally sourced clays. The identification of a production of western Greek wine (?) amphorae in Agrigento dating from the late 6th-4th century BCE breaks ground for a better understanding of the colony's economic development during the late Archaic and Classical periods. The city has to be regarded, in fact, as one of the major global players within the wider frame of Sicilian commercial interaction, especially during the 5th century BCE.

1. Introduction

This paper aims to completely characterise the archaeometric features of the western Greek amphorae series manufactured at *Akragas* from the late 6th-4th century BCE. Our investigation is based on detailed petrographic and chemical analyses of 21 samples of transport amphorae, 12 samples of coarse wares and three tiles, all hypothetically attributed to the production of *Akragas* on the grounds of archaeological considerations (see, Section 2). The studied materials are correlated to their complete archaeological records (morphological type, stratigraphical provenance, graphical documentation, dating, see Table 1) and have been petrographically and chemically compared with 12 local clayey samples outcropping in proximity to Gate III (Agrigento), which are reasonably considered potential points of supply for raw materials suitable to ceramic production (see, Table 2). The scientific issue of this interdisciplinary investigation will constitute a benchmark in view of a better understanding of Agrigento's role as one of the most important global players within the wider frame of economic and political interaction between Greek, Punic and native communities in Archaic and Classical-period Sicily (for similar studies: De Bonis et al., 2020; Montana et al., 2020).

The Greek colony of *Akragas* (present-day Agrigento), situated in the central part of Sicily's southern coast (Fig. 1A), was founded by nearby Gela around 580 BCE, possibly with the additional support of colonists from Rhodes and Crete. In 480 BCE, an alliance between *Akragas*, guided by its tyrant *Theron* (490/89–472 BCE), and Syracuse under *Gelon*

* Corresponding author at: Institut für Klassische Archäologie, Universität Wien, Franz Klein-Gasse 1, 1190 Wien.
E-mail address: babette.bechtold@univie.ac.at (B. Bechtold).
[1] These Authors contributed equally to this study.

https://doi.org/10.1016/j.jasrep.2022.103627
Received 18 May 2022; Received in revised form 1 August 2022; Accepted 28 August 2022

defeated the Carthaginians in front of Himera's western fortifications. As a result, *Theron*, and later his son *Thrasydaois* (472–471 BCE), extended Agrigento's supremacy over the Dorian-Chalcidian colony and large parts of northwestern Sicily until approximately 470 BCE (Vassallo, 2005). During the 5th century BCE, *Akragas* developed very quickly concerning its political and monumental organisation (Caliò, 2019). In connection with the renewed conflict between Carthage and the Sicilian cities during the last decade of the 5th century BCE, Agrigento was sieged and conquered by the troops of *Hannibal* in 406 BCE (Hans, 1983). The proceeding 4th century BCE probably represents a period of crisis, at least until the end of the century, when an urban reawakening can be noted (Caliò, 2019).

Agrigento belongs to the small selection of western Greek colonies explicitly mentioned by several ancient authors for their celebrated vineyards (van der Mersch, 1996; Brun, 2011; Scalici, 2019). Despite the likely prominent role of wine cultivation in Agrigento's territory, no systematic research has focused on identifying a local transport amphora series related to this lucrative commercial activity. However, recent excavations in several areas of the ancient city, predominantly the *kerameikos* outside gate V and south of the temple of Zeus, have produced some insight into the city's production of western Greek amphorae (Fig. 1B) from the late Archaic to the late Classical period (see, Sections 2.2-4).

The term "western Greek" denotes 6th-4th centuries BCE transport vessels manufactured by export-orientated Greek colonies of *Magna Graecia* and Sicily (latest: Gassner, 2015; Sacchetti, 2012; Sourisseau, 2011). In Greek Agrigento, pottery production was performed in at least two kiln areas located along the southern boundaries of the city, outside the Gates III and V (for the most recent overview: Baldoni et al., 2019). Specifically, excavations in this latter sector have allowed for the identification of five kilns A-E (see, Section 2.3).

Regarding archaeometric research, the first investigations (petrography and chemistry) were undertaken in the 90s on 74 ceramic samples of coarse wares, cooking wares, lamps, *terra sigillata* fine wares, and transport amphorae unearthed in the late Roman necropolis *subdivo* in Agrigento, and led to the hypothetic definition of a local group of coarse wares (Alaimo et al., 1995). One decade later, a team guided by G. Barone analysed four samples of western Greek amphorae, five samples

Table 2
Clay sampling.

Sample code	Sampling point	Description
AG-1	at the base of the gully under the *Tempio di Giunone*	whitish level
AG-2	under the *Tempio di Giunone*	yellowish-whitish level
AG-3	under the *Tempio di Giunone*	light yellow level
AG-4	under the *Tempio di Giunone*	yellowish level
AG-5	under the *Tempio di Giunone*	light grey level
AG-6	under the *Tempio di Giunone*	greysh level
AG-7	under the *Tempio di Giunone*	yellowish level
AG-8	at the base of the gully between the *Tempio di Giunone* and the *Tempio della Concordia*	yellowish level
AG-9	between the *Tempio di Giunone* and the *Tempio della Concordia* at about 20 m above the sample AG-8	yellowish level
AG-10	between the *Tempio di Giunone* and the *Tempio della Concordia,* 5–10 m above the sample AG-9	grey level
AG-11	taken from the top level, under the *Tempio della Concordia*	grey-yellowish level
AG-12	clayey hill just below the *Tempio della Concordia* (paleo-landslide)	grey-yellowish level

Table 1
Synopsis of data related to western Greek amphorae, coarse wares and tiles produced in Agrigento and provided with petrographic analysis. Typological identification of the amphorae referred to (Gassner, 2003 where '*Randform*' intends 'rim shape').

Discovery site	Site inventory	Inv. FACEM	Pottery type	Dating object	Chemistry	Published	Fig.
Himera	W5377	M 179/232	*Randform* 3	520–490	X	Bechtold 2020a, Fig. 1, 4	2C
Himera	RO1685	M 179/324	*Randform* 2	510–480	X	Bechtold 2020a, Fig. 1, 9	4E-F
Himera	W3047	M 179/332	*Randform* 3	480–460	X	Bechtold 2020a, Fig. 2, 3–4	5A-B
Himera	RO1339	M 179/287	*Randform* 4	470–450		Bechtold 2020a, Fig. 3,2	2A
Himera	W6194	M 179/233	*Randform* 6	450–420	X	Bechtold 2020a, Fig. 3,4–5	5D-E
Agrigento	AG 13/191	M 208/6	*Randform* 2	500–470			
Agrigento	QAV19.17.57	M 208/46	*Randform* 3	520–500			4A
Agrigento	QAV19.1.55	M 208/43	*Randform* 3	520–490		Baldoni, Scalici 2020, 12	4C
Agrigento	QAV19.13.20	M 208/45	*Randform* 3	520–490			
Agrigento	QAV19.15.7	M 208/47	Peg	520–480/70		Baldoni, Scalici 2020, 11	2B, 4D
Agrigento	QAV19.1.62	M 208/44	*Randform* 3	480–450		Baldoni, Scalici 2020, 12	5C
Agrigento	QAV19.8.1		*Close to Randform* 7	450–400	X		6A-B
Agrigento	QAV19.8.2		Body fragment		X		
Agrigento	AG 13/181/1	M 208/3	*Randform* 7	420/10–370	X	Bechtold 2020a, Fig. 4, 2	2D
Agrigento	AG 13/337/1	M 208/1	*Randform* 7	420/10–370	X	Bechtold 2020a, Fig. 4,1	6C
Agrigento	AG 13/200	M 208/5	*Randform* 7	380–340	X		6E
Agrigento	AG 13/337/2	M 208/2	*Randform* 7	380–340	X	Bechtold 2020a, Fig. 4, 4	6F
Selinunte	TR P13.107	M 154/143	*Randform* 3	510–480/70			4B
Selinunte	TB P08.550	M 154/111	*Randform* 3	480–450			
Selinunte	TR P12.179	M 154/123	*Randform* 7	380–340		Bechtold 2020a, Fig. 4, 6	6G
Pantelleria	PN06 ACR I 2079–3	M 119/174	*Randform* 7	420/10–370	X	Bechtold 2020a, Fig. 4,3	6D
Agrigento	AG 13/337/13/3	M 209/1	Lekane	4th BCE	X		
Agrigento	AG 13/191	M 209/2	Mortar	4th BCE			
Agrigento	AG 13/191	M 209/3	Mortar	4th BCE	X		
Agrigento	AG 13/183	M 209/4	Mortar	4th BCE	X		
Agrigento	AG 13/337/13/2	M 209/5	Lekane	4th BCE	X		
Agrigento	AG 13/337/5	M 209/6	Hydria	4th BCE	X		
Agrigento	AG 13/337	M 209/7	Handled bowl	4th BCE			
Agrigento	AG 13/337	M 209/8	Olpe	4th BCE			
Agrigento	AG 13/223/13	M 209/9	Olpe	4th BCE			
Agrigento	AG 13/337/8	M 209/10	Bowl	4th BCE	X		
Agrigento	AG 13/240/2	M 209/11	Lekane	4th BCE			
Agrigento	QAV19.16.49	M 209/13	Basin	510–450			
Agrigento	AG 13/183	M 210/1	Tile		X		
Agrigento	AG 13/183	M 210/2	Tile		X		
Agrigento	AG 13/183	M 210/3	Tile				

of coarse wares and one tile, all collected in the "western part of the temple valley", together with five ceramic samples from two medieval kilns found in the necropolis *subdivo* (Barone et al., 2003; Barone et al., 2004. Regrettably, the analysed pottery is not illustrated). The results of the analysis were compared with the data from the earlier coarse ware analyses (see above) and identified all ten samples as of local production. Ultimately, nine western Greek amphorae of presumed Sicilian production, yielded by the Agrigento-survey in the Monti Sicani, have been submitted to PIXE analyses (Klug, 2020).

2. Archaeological materials and methods

As with provenance studies conducted on western Greek amphorae mainly found in Himera (see, Section 2.1), but also discovered in several other Sicilian sites (for the project, see funding), ceramic samples chipped from freshly broken surfaces of nearly 1150 fragments were subdivided into macrofabrics by the use of hand lens. Thereon, all of the samples were analysed accordingly to the standardised methods implemented for the database of Fabrics of the Central Mediterranean (FACEM) and compared with reference samples of fabrics already defined by interdisciplinary, archaeological-archaeometric investigations. Petrographic research was conducted on representative selections of every macrofabric. Particular attention was paid to the identification and characterisation of Sicilian productions, and the first results were published in the eighth edition of FACEM.

Out of the ample *corpus* of ca. 1150 individuals., the study under a stereomicroscope of a selection of around 65 amphorae has led to the identification of a relatively homogeneous group (Fig. 2A-D), distinguished by a reddish-orange or sometimes yellow-greenish carbonatic matrix of rather fine texture (for the macroscopic description, see in detail: Ferlito, 2020). The majority of the studied items (N = 30 ca.) were found in Agrigento (Sections 2.2-2.4), 12 amphorae were unearthed in the necropoleis of Himera (Section 2.1), and a small group came from Selinunte, *Cossyra*/Pantelleria, Segesta, and Malta (Section 2.5) (Fig. 3). As a working hypothesis, this assemblage of western Greek amphorae has been attributed to the production of *Akragas*.

2.1. The amphorae found in the necropoleis of Himera

Extensive excavations were conducted during the 90s and from 2008 to 2018 by the Soprintendenza BB.CC.AA. (Beni Culturali e Ambientali) di Palermo in the western and eastern cemeteries of Himera (Fig. 1C-D). The excavations yielded ca. 13,400 tombs dating from the later 7th century BCE to 409 BCE, when the colony was destroyed and definitively abandoned (for the most recent update on this research, see: Vassallo, 2018). Nearly 5000 graves consist of *enchytrismoi*, that is to say, of burials of infants in large ceramic containers. In approximately 3100 cases, these vessels are represented by re-used transport amphorae, of which 556 items of this *corpus* belong to the western Greek type here under focus.

Based on archaeological fabric analyses according to the methods implemented for FACEM (see above), a selection of 12 amphorae has been tentatively ascribed to the production of Agrigento. Five items from this group were submitted to archaeometric analyses (Table 1). Only one burial from this ensemble (W6194/ M 179/233) was provided with a grave inventory.

Morphological studies have led to the distinction of three main shapes (previously, see: Bechtold, 2020a; Bechtold, 2020b):

- The earliest one, attested by six items and dating from the late 6th to the early 5th century BCE, includes globular-shaped or lenticular-shaped vessels with cylindrical pegs and short, straight necks. The semi-ovoid rims are rather thick with a maximum extension in the central part, often provided by an air chamber and strongly profiled at their inferior edges. This type corresponds to Sourisseau's form 2 (Sourisseau, 2011) and Gassner's *Randform* 3 (Gassner, 2003) (Fig. 4A, C). A minor selection of rims misses the external modulation, matching *Randform* 2 (Gassner, 2003) (Fig. 4E-F).
- Three heart-shaped amphorae reach their maximum diameter at the shoulder, have slightly convex necks, massive bottom-shaped pegs

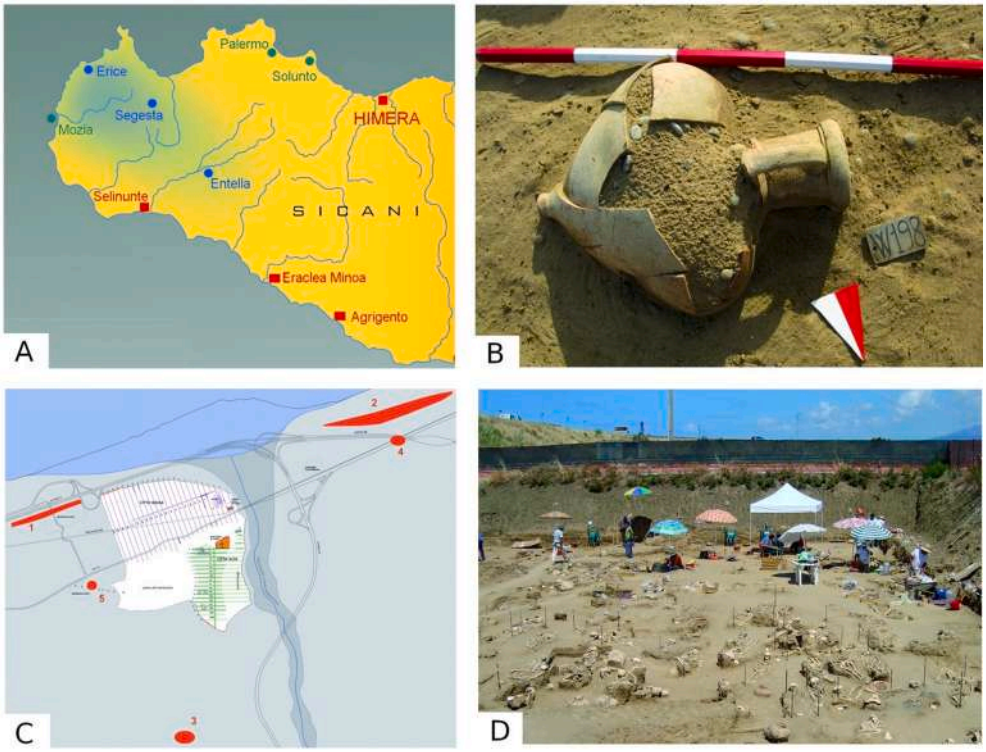

Fig. 1. (**A**) Geographical localisation of the main sites mentioned in this study; (**B**) western Greek amphora found in Himera; (**C**) planimetry of Himera; (**D**) excavations in the western necropolis of Himera.

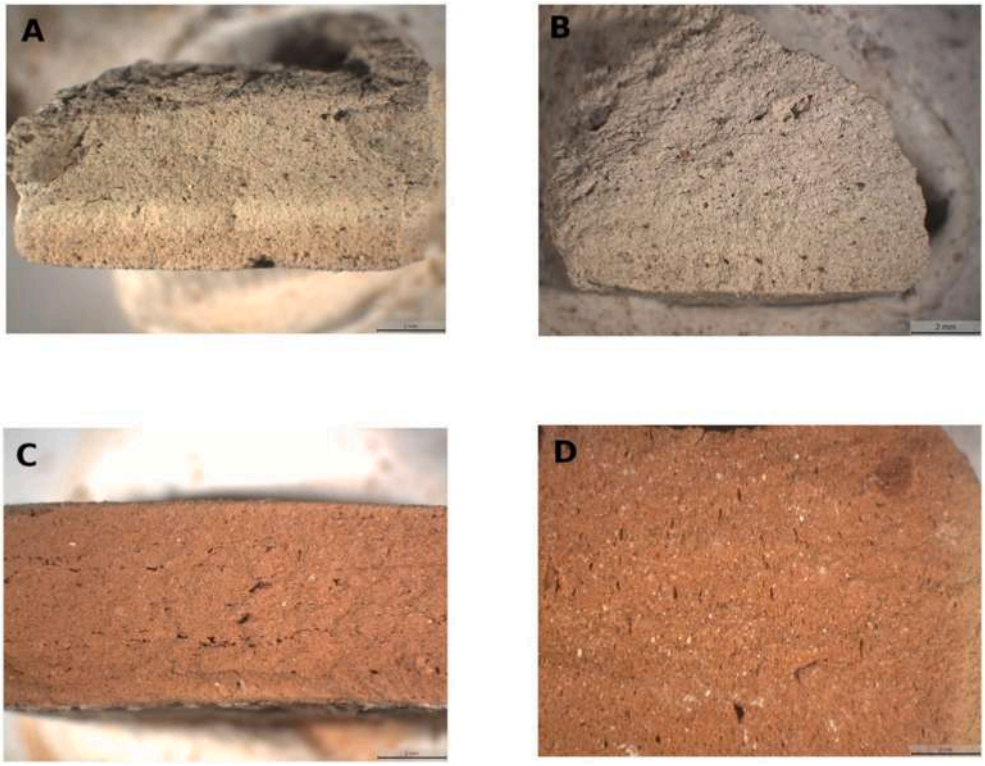

Fig. 2. Microphotos of fabrics of Agrigento at x8 magnification. (**A**) M 179/287; (**B**) M 208/47; (**C**) M 179/232; (**D**) M 208/3.

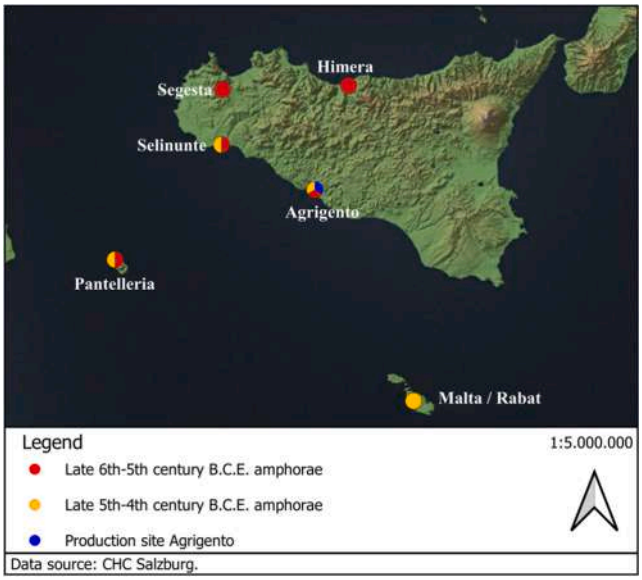

Fig. 3. The distribution of western Greek amphorae manufactured in Agrigento outside the production site (as at 2021).

and profiled, semi-ovoid rims with *Randform* 3. These probably represent the early Classical-period evolution of the late Archaic type above and date to the second quarter of the 5th century BCE (Fig. 5A-B).

- Finally, one amphora shows a pear-shaped body with a maximum extension at the shoulders and a characteristic, almond-shaped rim of *Randform* 6 (Gassner, 2003). It should be dated to the second half of the 5th century BCE (Fig. 5D-E).

2.2. The Amphorae, plain wares and tiles found in the area south of the temple of Zeus at Agrigento

Recent archaeological investigations in the years 2013–2015, undertaken by the Università degli Studi di Palermo in the area south of the temple of Zeus, have yielded considerable quantities of pottery. The ceramic finds stem mainly from stratified deposits related to the construction, use, and destruction of the so-called building 5, roughly dating to the late Archaic period and the mid/second half of the 4th century BCE (for a preliminary report, latest: de Cesare & Portale, 2017). In-depth typological studies have been conducted on all of the ceramic classes, which will be published in the final edition on the excavations. During this post-excavation phase, special focus has been placed on the macroscopic distinction of presumably local fabrics from imported artifacts. For this exact reason, the pottery from the present investigation has fulfilled all the conditions required for a supposed local control group, necessary in view of the archaeometric characterisation of the amphorae production of Greek *Akragas*. Therefore, a selection of eight amphorae fragments (Amico, 2020; Bechtold, 2020a), in addition to 14 fragments of coarse ware and three tiles, all of supposed local manufacture, has been submitted to the standardised archaeological documentation according to the FACEM-methods. Nineteen samples from this ensemble have undergone detailed petrographic and chemical analyses (Table 1). In relation to the transport amphorae, two fragments match the late Archaic globular type with *Randformen* 2–3 (as Fig. 4A-F), while six fragments represent different versions of a later 5th-4th century BCE shape (Bechtold, 2020a), characterised by semi-ovoid rims with their barycentre in the upper third and underlined by a ridge (Fig. 6C, E-F) close to *Randform* 7 (Gassner, 2003).

2.3. The amphorae and plain wares found the kiln area outside Porta V at Agrigento

Within a broad research project on the artisan production in Agrigento by the Università di Bologna, a new archaeological investigation

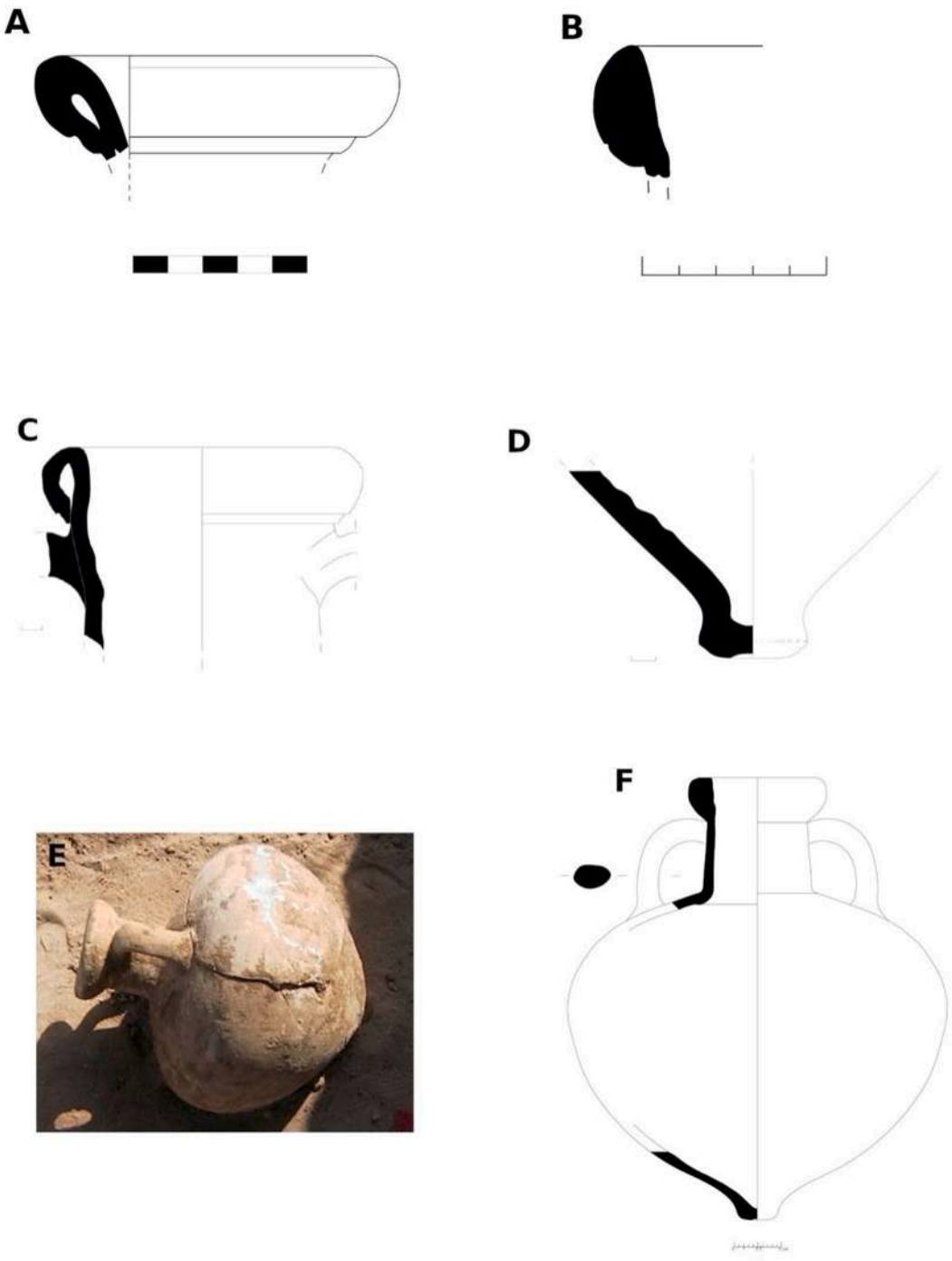

Fig. 4. Late Archaic amphorae produced in Agrigento. (**A**) M 208/46; (**B**) M 154/143; (**C**) M 208/43; (**D**) M 208/47; (**E**)-(**F**) M 179/324.

has been recently planned in the extramural sector located west of *Porta V*. This area is characterised by a privileged and particularly ideal location for artisanal activities. In fact, it is located close to the *Hypsas* river, the Sanctuary of the Chthonian Deities and the *Kolymbetra* basin, and it is functionally connected to *Porta V* and the important route axes of the polis. Materials and markers of ceramic production have been found in this area since the end of the 19th century. Unfortunately, it is nowadays not possible to associate those materials with any of the kilns which were discovered in the same area in the 20th century, where three kilns (a-c) were excavated, and a fourth kiln (D) was only superficially investigated (Baldoni, et al., 2019, with previous bibliography).

Starting in 2019 and still ongoing, the new archaeological explorations carried out by the Università di Bologna focused on kiln D and another kiln (E), located further South and identified thanks to the geophysical prospections conducted by the Bologna équipe before the beginning of the excavations in this area.

Both kilns D-E are characterised by their large size, although of different shape, construction technique and disposition: kiln D has a rectangular plan, it is partly excavated in the rock and its *praefurnium* faces south (Fig. 7); kiln E is excavated in the clay bank, and its *praefurnium* opens westward (Baldoni et al., 2019). The construction of the two D-E kilns appears to be chronologically consistent with the building of the polis walls and the monumentalisation of the sacred area in the Late Archaic period. Based on the materials produced and the few imported finds, it is currently assumed that the two D-E kilns were used until approximately the middle of the 5th century (Baldoni et al., 2019).

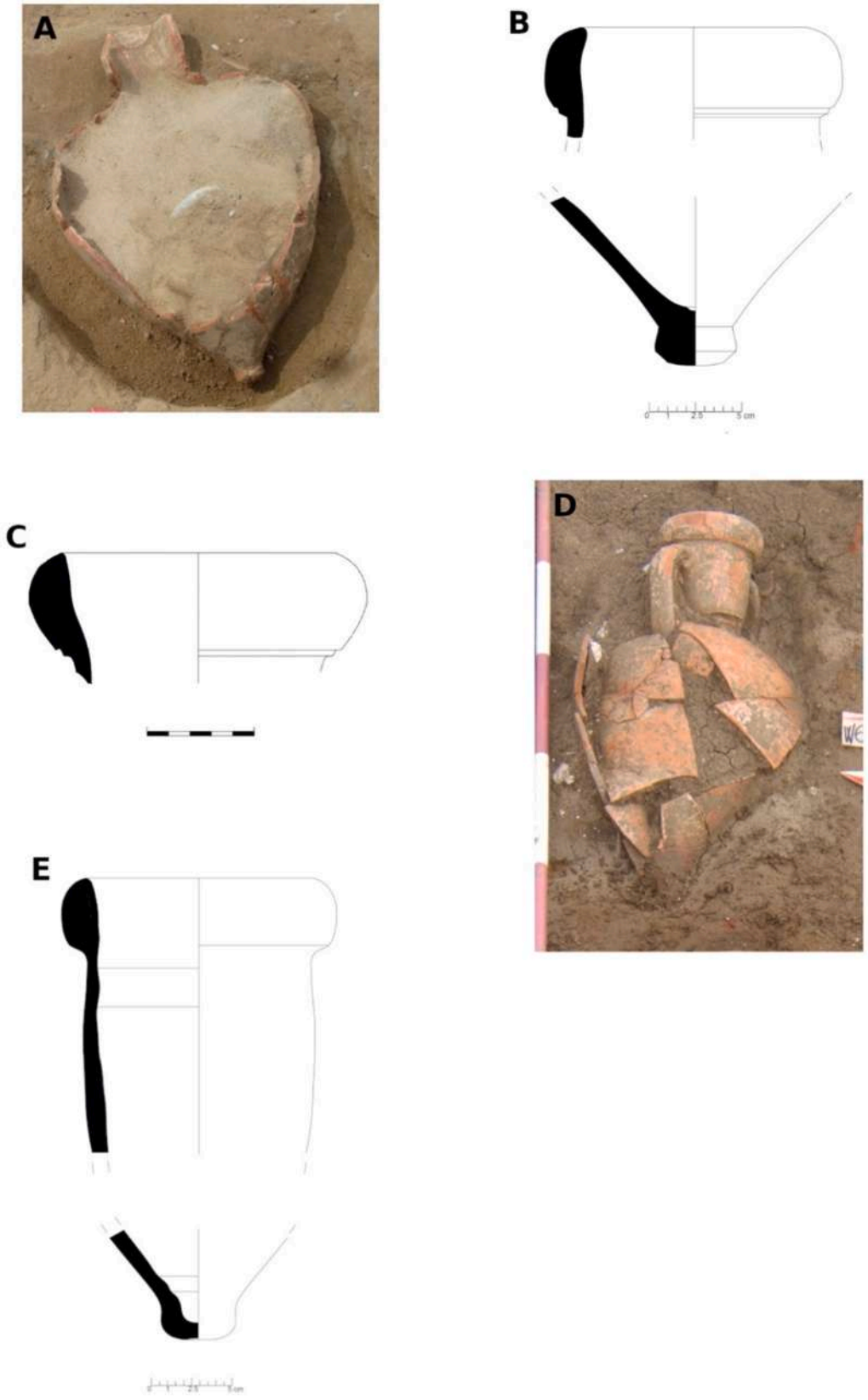

Fig. 5. Classical-period amphorae produced in Agrigento. (**A**)-(**B**) M 179/332; (**C**) M 208/44; (**D**)-(**E**) M 179/233.

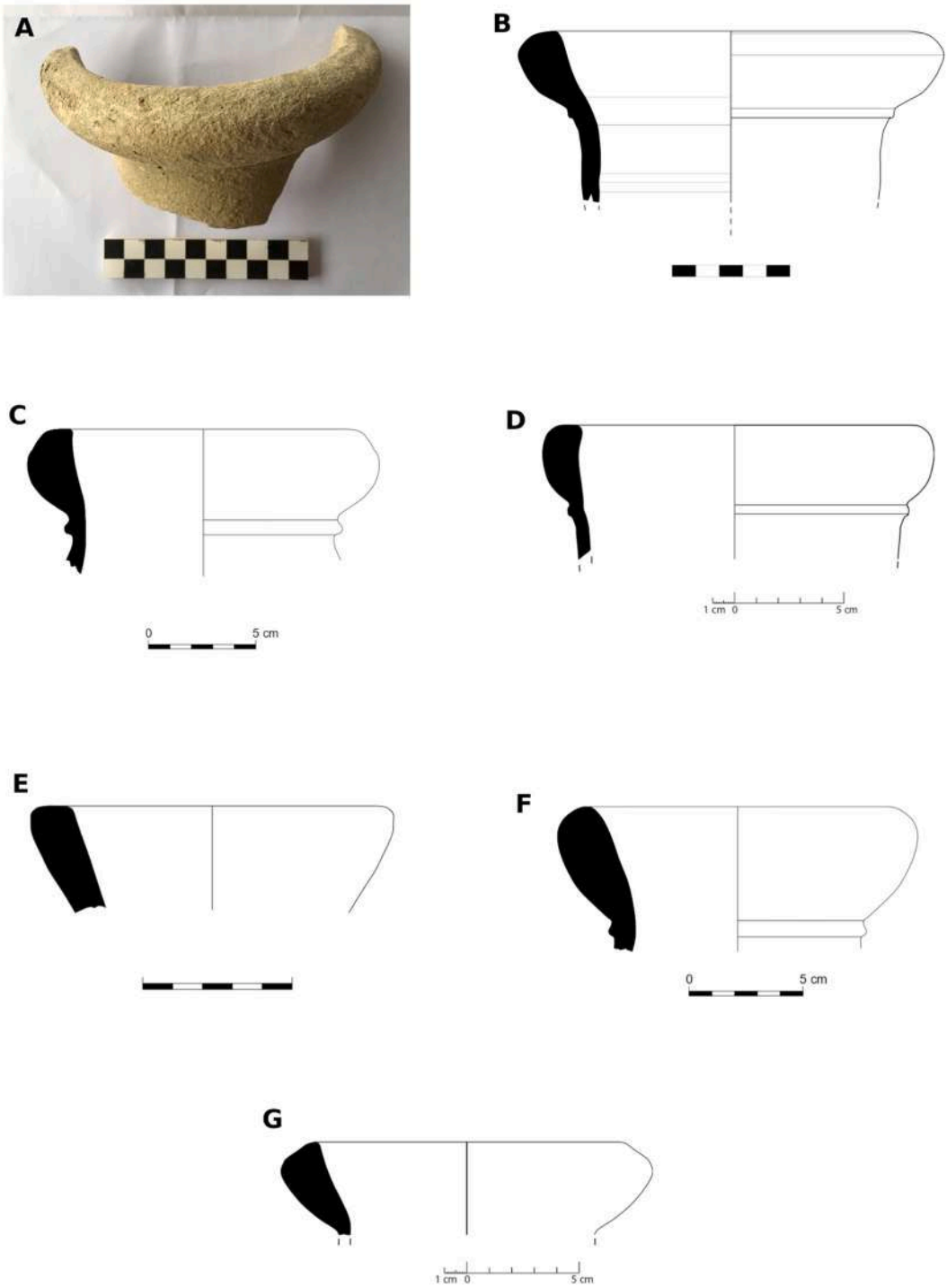

Fig. 6. Late Classical amphorae produced in Agrigento. (**A**)-(**B**) kiln waster QAV19.8.1; (**C**) M 208/1; (**D**) M 119/174; (**E**) M 208/5; (**F**) M 208/2; (**G**) M 154/123.

For the first time, new investigations enabled the certain documentation of material produced in these two kilns, from which come tools for production (spacers and supports), coarse ware, cooking ware, fine ware, tiles and a very considerable group of commercial amphorae of the western Greek type, including many wasters (Baldoni et al., 2019; Baldoni & Scalici, 2020). The typological study of the finds was supported by petrographic analysis of several classes produced, especially on the commercial amphorae (first mentioned in Baldoni & Scalici, 2020; Bechtold, 2020a).

The amphorae, which have the same fabric as the common pottery, are produced in both kilns D-E. Most of the sherds can be attributed to *Randform 3*. However, several variants have been identified, which are assumed to correspond to different periods of production: an older (more numerous) late Archaic type and a more recent, less frequent and slenderer one, dating to the mid-5th century or shortly after (Scalici in Baldoni & Scalici, 2020).

The fragments subjected to petrographic analysis (Table 1) come from the surface layers (UUSS 1, 16, 17), the fills of the kilns (UUSS 13), and external areas (US 15). Among them are amphorae of the late Archaic type (M 208/46, Fig. 4A; M 208/43, Fig. 4C; M 208/47, Fig. 4D) and of the early Classical-age variant (M 208/44, Fig. 5C). In addition, two wasters, a wall fragment, and a rim fragment of commercial

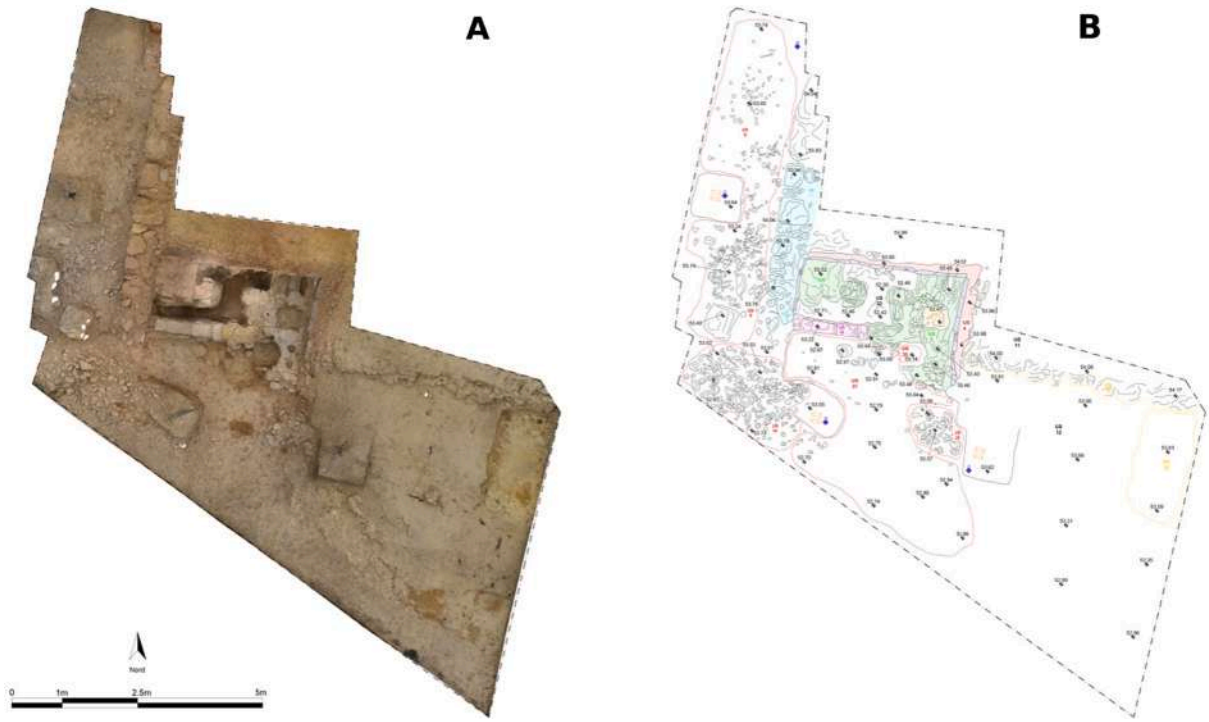

Fig. 7. Photomap (**A**) and plan (**B**) of kiln D (after Baldoni, Parello, Scalici 2019, Fig. 6; authors: S. Schillaci, U. Orlando).

amphorae (Table 1) were examined petrographically and chemically. They were found in a superficial layer in the external area northwest of kiln D, between the latter and kilns B-C (US 8). Because of its thickened upper part and the ridge which has shifted down to the beginning of the neck, the rim fragment QAV.19.8.1 (Fig. 6A-B) seems already close to the selection of *Randform* 7-items (see Fig. 6, C-D, G) of the late Classical period (see, Section 2.2). Although it is not possible to establish its specific context of provenance, the presence of this finding could confirm the existence of a production of commercial amphorae in some kiln located in the artisanal area west of *Porta V* in the late Classical period, as has already been suggested in the past (Baldoni et al., 2019: 114-115, with previous bibliography).

2.4. The amphorae found in the Hellenistic-Roman sanctuary at Agrigento

Since 2013, a joint mission composed of the Università di Catania, the Politecnico di Bari and the Parco Archeologico di Agrigento has been conducting excavations in the Hellenistic-Roman sanctuary located in the vicinity of the *agora* (Caliò et al., 2016). Within the framework of the project on western Greek amphorae (see funding), the present author had the opportunity to sample and study a small selection of seven rim fragments of presumable local production, yielded by the 2017-campaign conducted in the area of the northern *porticus*. All items were residual finds in Hellenistic or Roman deposits and refer to the late Archaic, globular type with *Randformen* 2–3 (as Fig. 4A-F).

2.5. The amphorae found in Selinunte, Segesta, Cossyra/Pantelleria and Malta

The last group includes amphorae hypothetically originating from Agrigento but found outside the production site. A small selection of five fragments has been yielded by the Institute of Fine Arts/NYU – Università degli Studi di Milano-excavations in the major urban sanctuary of Selinunte, around temples B and R (Marconi, 2014; Marconi, et al., 2017). Three fragments of this group have been submitted for archaeometric analyses (Table 1). All of the items represent residual finds included in early Hellenistic layers. Three amphorae refer to the globular late Archaic shape (as Fig. 4A-F), whilst respectively-one fragment belongs to the successive early (as Fig. 5A-C) and late Classical shape (Fig. 6G).

Seven fragments stem from the acropolis excavations and the suburban survey of *Cossyra* undertaken by the Universität Tübingen (Schäfer et al., 2015 with further references), one of which has undergone archaeometric research (Table 1). The amphorae, presumably to be attributed to the production of *Akragas*, are all residual finds from later contexts. One item belongs to the late 6th-first half of the 5th-centuries BCE shape (as Figg. 4, 5A-C), while six items match the late Classical type with *Randform* 7 (as Fig. 6A-G).

The fragments from the following last two sites have not yet been submitted for archaeometric analyses. Their attribution to the production of *Akragas* is based on archaeological fabric studies according to the FACEM-method. Four amphorae have been identified amongst two ritual contexts of Segesta: the "Grotta Vanella dump" and the Mango sanctuary (fragments published in: de Cesare et al., 2020). Three items belong to the globular, late Archaic type (as Fig. 4), and the fourth might refer to the early Classical shape (as Fig. 5A-C). Finally, a single amphora rim from Rabat/Malta (unpublished, from GHX2013: Excavations of the Superintendency of Cultural Heritage of Malta under the direction of N. Cutajar) has been attributed to the late Classical type with *Randform* 7 (as Fig. 6A-G).

3. Geological context and raw clay sampling

The territory of Agrigento is located in the southern-central sector of an important regional tectonic structure named "Caltanissetta synform" (Catalano et al., 2013). The rocks outcropping in this sector consist of Miocene deposits pertaining to the *Gessoso Solfifera* series which are covered by Plio-Pleistocene marly clay and biocalcarenites. The main morphological reliefs, aligned along the NW-SE direction, match with the main axial culminations of the plicative system that characterises the deformative pattern of this sector of the Sicilian chain. This deformation is responsible for the alternating and variable distribution of clayey outcrops moving along the NE-SW direction.

The area of the *Valle dei Templi* is characterised by the extensive outcrop of lithotypes with high contrasts of competence that generate important morphologies inherited from differential erosion processes. Generally, the yellowish Pleistocene biocalcarenites, which form the substrate on which the Archaeological Park is located, rest in a continuity of sedimentation above the Upper Pliocene-Lower Pleistocene grey marly-clayey. In detail, the Pleistocene outcrops are characterized by three main facies: (A) yellow clayey-sandy silts; (B) gray marly sands; (C) biocalcarenites and biocalcirudites (Cotecchia et al., 2005). The facies A and B, that crop out at the base of the southeastern slope below the *Tempio di Giunone*, contain a level rich in planktonic foraminifera (e.g. *Globorotalia inflata*), which alternate at the level with marine mollusks (e.g. *Arctica islandica*) and allow the attribution of these deposits to the lower Pleistocene age (Fig. 8). Clay sampling was carried out in the gullies between the *Tempio di Giunone* and the *Tempio della Concordia*, just below Gate III (Fig. 9A-B). 12 samples were collected at different points located at various altitudes along the gullies, in order to evaluate significant differences along the stratigraphic succession, for the purpose of using the material as a ceramic raw material. (Table 2). About 2 kg of clayey material was collected after removing the most superficial part, even if the lack of a *stricto sensu* soil level on this type of geological deposit is evident (Fig. 9C-D). This quantity has been subjected to drying and quartering (following the procedures illustrated in the next paragraph) for the subsequent selection of the aliquots to be addressed to the various analytical routines, i.e. grain-size distribution, X-ray powder diffraction and thin section-microscopy (after experimental firing test).

4. Experimental procedures and analytical methods

Minero-petrographic observations on the thin section obtained from the selected amphora samples were carried out through a Leica DM LSP polarizing microscope equipped with a digital camera (Leica DC 200). The relative abundance of non-plastic inclusions (expressed as area %) was determined by conventional point-counting procedures and comparative tables (Matthew et al., 1991). Microscopic observations

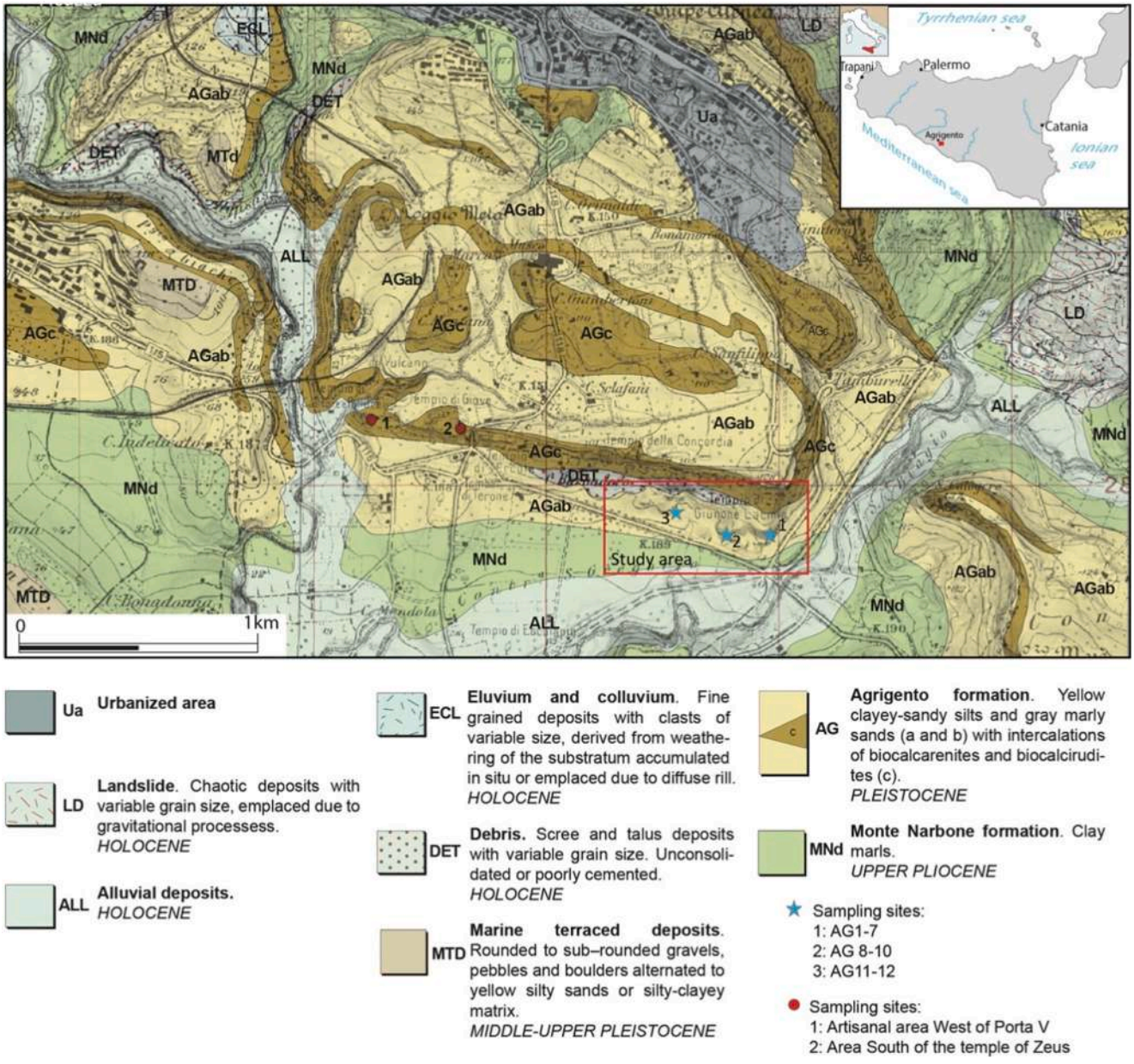

Fig. 8. Geological map of the studied area (modified after Bigi et al., 1972).

Fig. 9. Clay sampling along the Valle dei Templi: (A) clay slopes beneath the Tempio di Giunone and Tempio della Concordia (B); stratigraphic sampling along the clay slopes by the Tempio di Giunone (C); collecting sample AG-8 (D).

were carried out also on clay samples collected in the *Valle dei Templi*. A proper quantity of air-dried clay (50 g) was disaggregated, homogenized and mixed with water until optimal plasticity was achieved. Small briquettes were then made using wooden formwork (two for each sample, with dimensions 40x15x15 mm). They were in turn dried in a ventilated oven at 60 °C and formerly fired in a muffle furnace at 700 °C and/or 900 °C. The resulting firing tests have been embedded in epoxy resin and thin sectioned to be observed under the polarizing microscope (Montana, 2020).

Clay samples were first placed to dry in the laboratory at room temperature for 1–2 weeks and then gently crushed in a porcelain mortar. At the end of these pre-treatments, after careful quartering, the proper amount was put through grain size analysis. Samples were first separated into a coarse fraction (particles between 2 and 0.06 mm) and a fine fraction (particles < 0.06 mm) in a settling cylinder according to Stokes' Law. The fine fraction suspension was further separated into silt (0.06–0.002 mm) and clay (<0.002 mm) via centrifugation cycles at 2000 rpm and 4000 rpm, respectively. The different particle size fractions were dried in a ventilated oven at 60 °C for 48 h, stabilized at room temperature in a silica gel dryer, and then weighed with an analytical balance (Montana et al., 2012; Montana, 2020).

X-ray powder diffraction (XRPD) was only carried out on two representative clay samples (AG-1 and AG-11), whose experimental briquettes were selectively fired at 120 °C, 600 °C, 700 °C and 900 °C. Powdered bulk clay samples, both at natural state and after experimental firing, were obtained by grinding using an agate mortar. A PANanalytical X'PERT PRO diffractometer was employed, with the following operating conditions: Cu anode, graphite monochromator, 40 kV and 30 mA, 5°–60° 2θ scan range, 2° 2θ min–1 scan rate and 2 s time constant.

Bulk chemical data of selected ceramics (19 samples) and clays (7 out of 12) were determined at Activation Laboratories ltd (Ontario, Canada), using the fusion inductively coupled plasma optical emission spectrometry (ICP-OES) technique for major oxides and inductively coupled plasma mass spectrometry (ICP-MS) for trace elements. Samples were first air-dried, ground, and homogenized in a planetary agate ball-mill (Retsch PM100). Samples were prepared and analysed in a batch system. Each batch contains a method reagent blank, certified reference materials and some replicates. Samples were mixed with a flux of lithium metaborate and lithium tetraborate, and fused in an induction furnace. The molten melt was immediately poured into a 5 % nitric acid solution containing an internal standard until completely dissolved. The samples were run for major oxides and selected trace Varian Vista 735 ICP. Calibration is performed using seven prepared USGS and CANMET certified reference materials. One of the seven standards was used for every group of 10 samples during the analysis. Fifty-five elements were considered (10 major elements and 45 trace elements). The results concerning major elements (Si, Al, Fe, Mn, Mg, Ca, K, Na, Ti, and P) were normalized on a dry-weight basis and were given as a weight % of the corresponding oxides, with a detection limit of 0.01 % weight, except for MnO and TiO_2 whose detection limit is equal to 0.001 % weight. Trace elements concentration were expressed as parts per million (ppm) and the corresponding detection limit being specified between brackets: Sc (1 ppm), Be (1 ppm), V (5 ppm), Ba (2 ppm), Sr (2 ppm), Y (1 ppm), Zr (2 ppm), Cr (20 ppm), Co (1 ppm), Ni (20 ppm), Cu (10 ppm), Zn (30 ppm), Ga (1 ppm), Ge (1 ppm), As (5 ppm), Rb (2 ppm), Nb (1 ppm), Mo (2 ppm), Ag (0.5 ppm), In (0.2 ppm), Sn (1 ppm), Sb (0.5 ppm), Cs (0.5 ppm), La (0.1 ppm), Ce (0.1 ppm), Pr (0.05 ppm), Nd (0.1 ppm), Sm (0.1 ppm), Eu (0.05 ppm), Gd (0.1 ppm), Tb (0.1 ppm), Dy (0.1 ppm), Ho (0.1 ppm), Er (0.1 ppm), Tm (0.05 ppm), Yb (0.1 ppm), Lu (0.01 ppm), Hf (0.2 ppm), Ta (0.1 ppm), W (1 ppm), Tl (0.1 ppm), Pb (5 ppm), Bi (0.4 ppm), Th (0.1 ppm), U (0.1 ppm).

5. Results

5.1. Clays

5.1.1. Granulometric analysis

Grain size analysis of the twelve local clay samples showed evidence of a good textural homogeneity, even if collected at different points of the exposed outcrop, from the bottom to the top. The only exception regards a certain degree of variability in the relative abundance of the sand fraction (0.06–2 mm) for the samples AG-1 and AG-2. In fact, 10 out of a total of 12 analysed clay samples are characterised by sand

contents ranging from 2 to 9 % by weight (Table 3). Only the samples coded AG-1 and AG-2 showed comparatively greater fine sand amounts (averagely 15 % weight). In general, based on their average values, the sampled raw material exhibited a comparable amount between clay (average 45 % wt) and silt (average 47 % wt) fractions. Looking at the granulometric data concerning the finest components, samples AG-7 and AG-10 were those in which the clay particles (<0.002 mm) prevailed over the silt (0.002–0.06 mm), regardless of the relative abundance of sand (apparently fewer in AG-10). In contract, silt slightly overcomes the clay-sized particles in the remaining samples. The projection of the values obtained through the granulometric analysis on Shepard's ternary diagram 1954 allowed the classification of the studied materials as silty clays, except for sample AG-2, which was classified as a silty clay loam (Fig. 10).

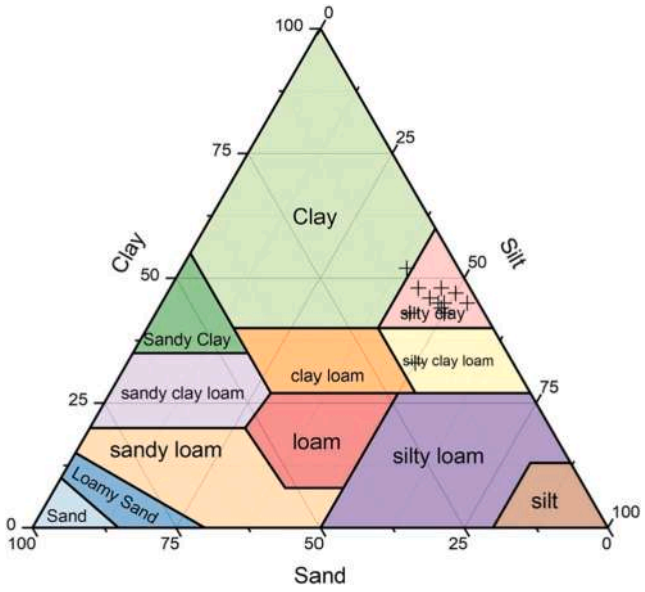

Fig. 10. Ternary diagram for granulometric classification of the raw clay samples.

5.1.2. *Petrographic characterisation of firing tests*

Textural and compositional features (microfabric) observed after firing tests on raw clay have been summarised in Supplementary Materials S1. In general, all the sampled clays showed a substantial similarity in textural (i.e. relative abundance, morphology and size distribution of aplastic grains) and mineralogical composition (i.e. monomineralic grains, rock fragments and bioclasts). They are characterised by good sorting and comparable relative abundances of aplastic grains, ranging between 10 and 20 % area. These latter are absolutely tiny, mainly falling in the classes of coarse silt (0.04–0.06 mm) and very fine sand (0.06–0.125 mm). Granules with medium sand size (0.25–0.5 mm) are sporadic, while those with a diameter greater than 0.5 mm are rare. The most abundant mineralogical phase is monocrystalline quartz, while polycrystalline quartz, feldspars, and mica flakes are less common or sporadic to rare constituents. Calcareous microfossils are also abundant or common constituents, being mostly decomposed after the firing process and replaced by micrite clots and/or pore casts (Cau Ontiveros et al. 2002). Among the accessory phases, anhydrite (originating from gypsum transformation after firing at 700 and/or 900 °C), glauconite, iron oxides and pyrite framboids equally characterise all the samples (Fig. 11). The groundmass of all the studied firing tests was generally optically inactive (only weakly active for those carried out at 700 °C) and characterised by homogeneous texture, without evidence of clay lumps.

5.1.3. *X-ray powder diffraction and chemical analysis*

Given the compositional and textural homogeneity of the fired clay briquettes, the mineralogical analysis by X-ray powder diffraction (XRPD) was carried out on only two selected samples (AG-1 and AG-11), respectively representative of the bottom and the top of the outcrop, and showing the greatest mutual variability in term of sand contents. Both samples showed the presence of calcite (slightly more abundant) and quartz constituting sand and silt fractions, together with much smaller quantities of feldspars and gypsum. The clay-sized fraction was mainly composed of illite and kaolinite with negligible swelling clay minerals. Some mineralogical transformations have been recorded after firing at increasing temperatures. In particular, the first change was soon observed at 120 °C (both AG-1 and AG-11) when gypsum ($CaSO_4{\cdot}2H_2O$) started its heat-driven transition to the anhydrous phase ($CaSO_4$, anhydrite), through the appearance of calcium sulphate hemihydrate ($CaSO_4.0.5\ H_2O$, bassanite). At about 600° C, anhydrite almost completely replaced bassanite (which remained metastable only in traces) and kaolinite collapsed its structure. Only illite between the clay minerals resisted up to about 800 °C. At 900 °C, calcite collapsed as well, while the newly formed mineral phases, like Ca-rich feldspar, Ca-pyroxene and hematite started coming into court. It is to be noted that illite traces remained in the sample AG-11, even at temperatures above 800 °C (Fig. 12).

Table 3
Granulometric analysis of clay samples.

Sample code	Sand	Silt	Clay
AG-1	13	44	43
AG-2	17	50	33
AG-3	8	46	46
AG-4	7	48	45
AG-5	7	50	43
AG-6	6	49	45
AG-7	9	43	48
AG-8	7	49	44
AG-9	9	39	52
AG-10	5	47	48
AG-11	2	53	45
AG-12	3	50	47

The chemical composition of the analysed clay samples is reported in Table 4. A reasonable compositional homogeneity is also evident from the results of the chemical analyses of the local raw clays, reflecting the previously described mineralogical and textural features. As can be seen, all the analysed samples showed an average CaO content close to 13 % weight and, according to the definition of Maniatis and Tite (1981), they can be classified as "calcareous clays". It should be noted that the variation range of CaO is slightly wide (9.79–17.21 %, CV equal to 20 %). This result could be related to the natural variability in the relative abundance of calcareous microfauna along the stratigraphic succession (as frequently observed in marine clay deposits) and/or to the variability of detrital gypsum. A lower variability is evident for all the other major oxides with CV within 10 % or sometimes lower than 5 %. Sodium and phosphorus oxides are an exception as both exceed 10 %. The satisfactory compositional homogeneity has also been observed for trace elements. The coefficient of variation (CV) of the most significant elements (in terms of geochemical connotation) is generally below 10 % (i.e. V, Y, Cr, Rb, Nb, HSFE) and sometimes between 10 and 20 % (i.e. Ba and Zr). Only in the case of Sr, an element geochemically related to Ca, has a wider range of variance been observed (CV > 20 %).

5.2. *Ceramics*

5.2.1. *Thin section petrography*

As described previously in Section 2, the set of 36 ceramic samples objected to thin section microscopy examination was already thought to have been produced at Agrigento (Fig. 8, red dots 1–2, Table 1) based on archaeological fabric studies according to the standardised methods of FACEM (see, Section 2). Therefore, the main purpose of polarising

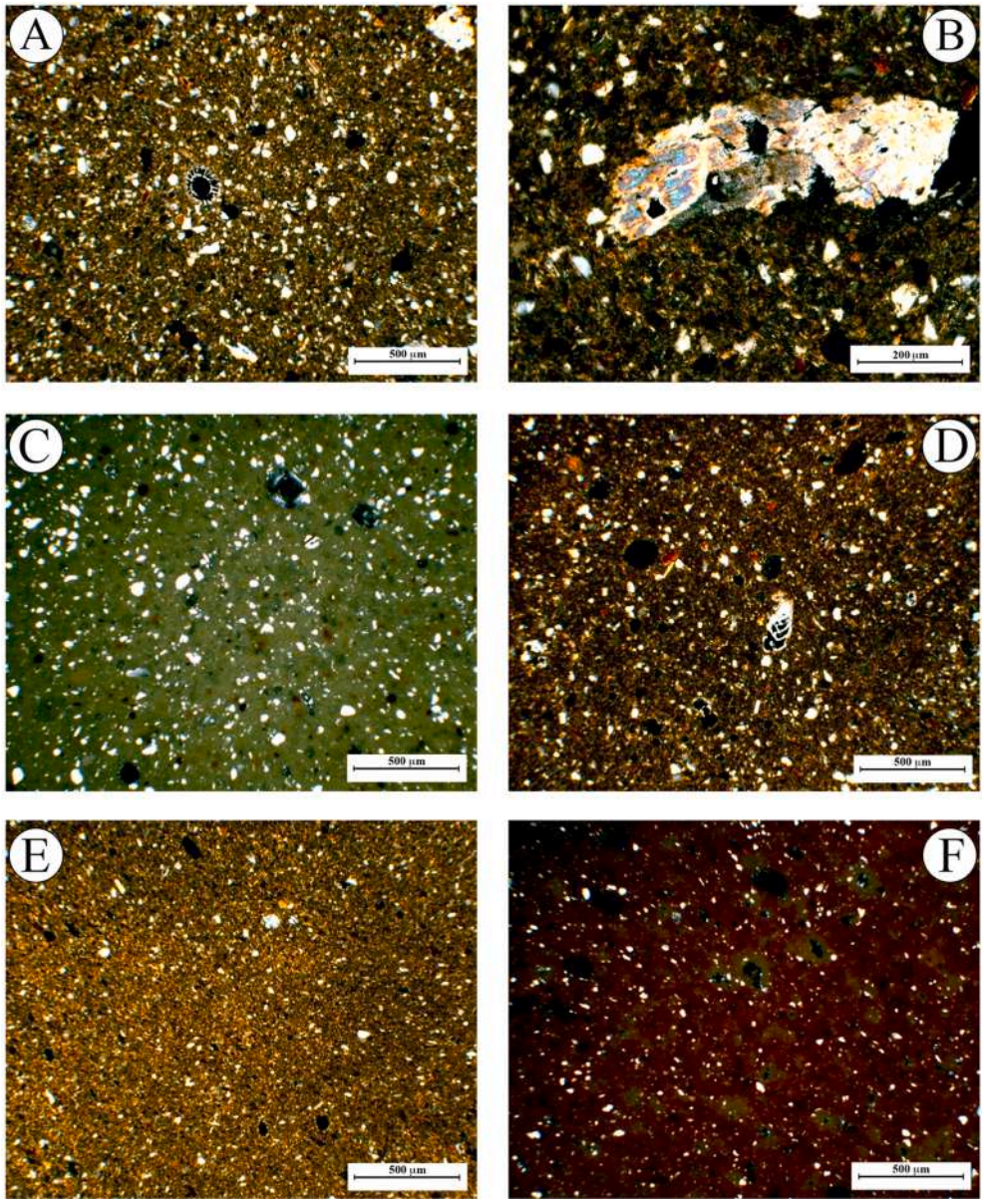

Fig. 11. Thin section microphotographs of clay samples after experimental firing test at 900 °C (XPL): (A-F) overview of the textural and mineralogical aspects; (B) details of anhydrite crystals originated by gypsum dehydration after firing.

microscope observation was not merely to confirm the supposed provenance, but rather to evaluate the homogeneity of this "paste group". To achieve this goal, compositional and textural features of aplastic inclusions (packing, sorting, size distribution, nature of monomineralic grains and lithic fragments) have been carefully evaluated and compared with those (previously described) found in local clayey raw materials after experimental firings at 700 and 900 °C.

It is considered opportune to state that microscopic observations ascertained the homogeneous petrographic characteristics of the considered ceramic samples. Their compositional and textural characteristics are covered in detail in Supplementary Materials S2, S3 and S4. Agrigento's pottery microfabric, in general, is characterized by the serial distribution of aplastic inclusions. They are mainly sized between coarse silt (0.04–0.06 mm) and fine sand (0.125–0.25 mm), and grains greater than 0.3 mm are sporadic to rare. Aplastic abundance (packing) varies from medium (10–15 % area) to medium/high (15–25 % area). The siliciclastic component showed the same abundance as the calcareous one. This latter is represented by bioclasts (from partially to fully decomposed after the firing process), micritic clots (Cau et al., 2002) and, indirectly, by the corresponding cast pores. Monocrystalline quartz is the main component, followed by common polycrystalline quartz, while feldspars are sporadic to rare. Mica flakes are also sporadic to rare constituents except for sample M179/332 (common). Siliceous lithoclasts and glauconite are rare as well. Iron oxides / hydroxides are accessory constituents, mainly concentrated as lumps scattered in the groundmass. It should be noted that rare anhydrite crystals were highlighted only in samples M 209/8 and M 179/332. The groundmass of all the analysed samples is optically inactive and characterised by sporadic to rare lumps (Fig. 13A-E).

The assignment of these archaeological finds to a single mineropetrographic "paste group" (MPG) allows them to be considered as originating from the same raw clay source and similar production processes. This last assertion is supported by the excellent correlation found between the ceramic microfabric and those obtained from experimental firing of the clays available at a short distance from the recently discovered furnaces (see for comparison the microfabrics shown in Fig. 9 and described in detail in Table S1). Even the production wasters found during the excavations of the kiln areas located along the southern

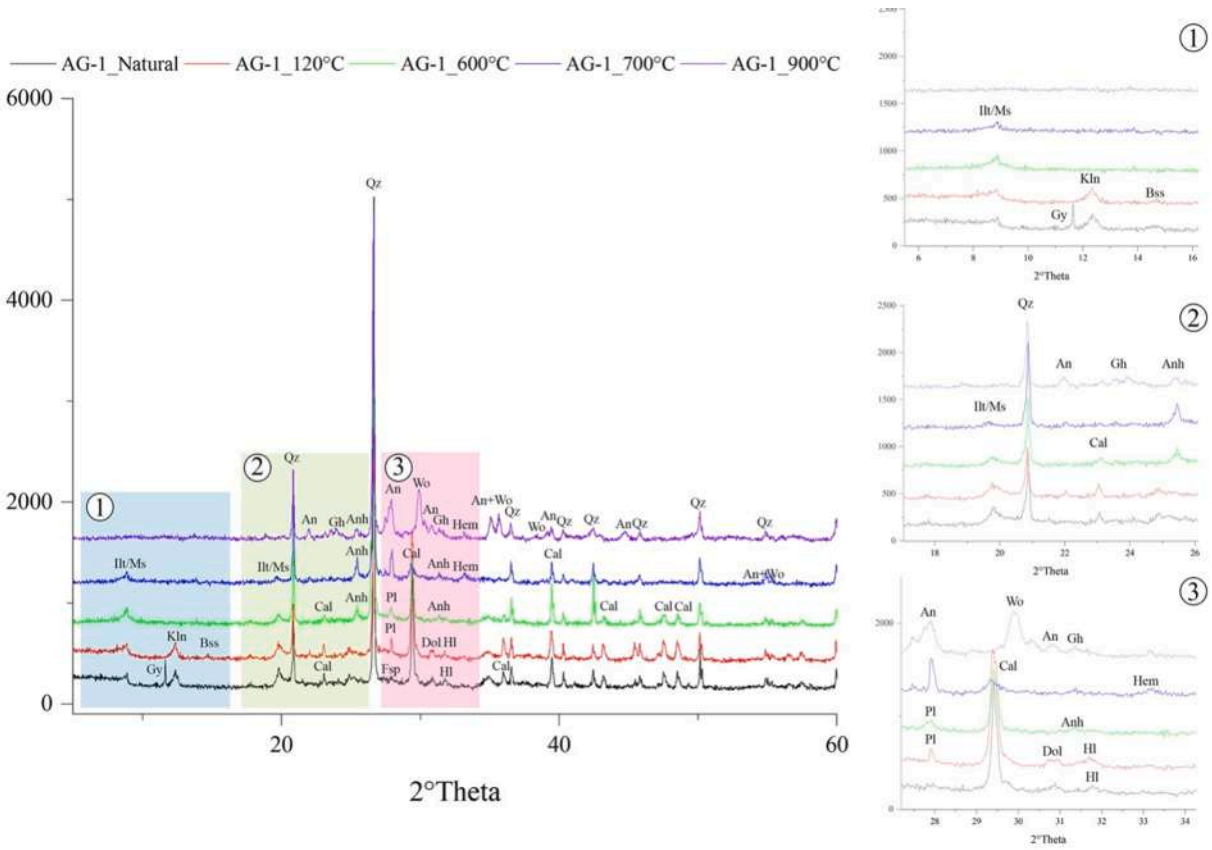

Fig. 12. XRPD patterns of representative Agrigento clay after experimental firing at different temperatures. Legend: Qz = quartz, Cal = calcite, Ilt/Ms = Illite/Muscovite, Gy = gypsum, Bss = bassanite, Kln = Kaolinite, An = Anorthite, Anh = anhydrite, Wo = wollastonite, Fsp = feldspar, Pl = plagioclase, Hem = hematite, Dol = dolomite, Gh = gehlenite, Hl = halite.

boundaries of the city, and subjected to petrographic analysis, fit the described microfabric satisfactorily (Fig. 13F). Finally, this petrographic description confirms and enriches with details what has already been noted in previous studies, concerning other ceramic productions attributed to the Agrigento furnaces (Alaimo et al., 1995; Barone et al., 2004).

5.2.2. Chemistry

The chemical compositions of the group of amphorae selected as local productions are shown in Table 5, together with those relating to the two kiln wasters (samples QAV-1 and QAV-2).

From a first examination of the data, it can be seen that the values of the coefficient of variation (CV) are well below 10 % or quite close to this threshold for most of the major elements' oxides, including CaO (CV = 13.72 %). Therefore, the set of samples can be considered acceptably homogeneous also from the point of view of the chemical composition. The only exceptions are represented by MnO (CV = 21.33 %) and Na_2O (CV = 23.54 %). In the case of manganese, considering that the absolute concentrations are very low and close to the instrumental detection limit, the variability could be considered "physiological". On the other hand, sodium can be imagined as derived from a variable level of contamination by NaCl in the local raw clays. In this regard, the anomalous sodium content of local clays was highlighted in the previous paragraph (average value 1.74 % by weight and CV = 17.12 %), and it can be compared to what is normally found in Sicilian Neogene clays, i.e. values, sporadically over 0.5 % by weight (after Montana, 2011). In this specific case, the anomalous contents (average value = 0.96 % weight for local amphoras and 0.81 % weight for kiln wasters) could be related both to the relative proximity to the sea (a few kilometres as the crow flies) and also to the presence of detrital material deriving from the *Gessoso-Solfifera* Formation (Schreiber et al., 1976), as already highlighted for interpreting the presence of gypsum in natural clays and bassanite / anhydrite in the associated experimental firing tests. The ceramic production process could involve water treatments of the clayey raw material as a preliminary procedure, which, consequently, could lead to a consistent NaCl washout (NaCl solubility equal to 360 g per litre of pure water at T = 25° C). This could explain the non-negligible differences in the concentration of Na_2O between local clays (1.74 % by weight) and local ceramic products (0.96 % by weight).

Considering the other more significant major elements, SiO_2 has an average value of 59.02 % by weight and a relatively limited variation range (55.79–61.34 %). The same can be said for Al_2O_3, Fe_2O_3, MgO and K_2O, which show average values respectively of 13.61 %, 5.68 %, 2.20 % and 2.09 % by weight, all satisfactorily similar to what was found in local clayey materials and kiln wasters. Calcium is the only major element that shows a non-negligible dispersion of the concentration values (range of variation 10.96–18.70 % in weight) compared to an average value of 15.29 % in weight. While for the local clays, a correlation between CaO concentrations and the content of calcareous microfauna and/or the presence of gypsum deriving from the evaporitic formations has been highlighted (average concentration of CaO = 12.54 %). The same variability in the ceramic finds also seems to be affected by the precipitation of secondary calcite during the burial phase. Petrographic observations confirmed this hypothesis, revealing the frequent presence of secondary microcrystalline calcite and explaining the higher average value in the ceramic artefacts compared to local raw clays.

Even in the case of trace elements the majority of the variation coefficients (CV) are well below 20 %, which is the threshold value below which the dispersion of trace values can be considered acceptable. Barium stands out among the most interesting elements, such as

Table 4
LOI normalized chemical composition of the clay samples.

Element Oxide (wt%)	AG- 1	AG- 5	AG- 6	AG- 8	AG- 9	AG- 10	AG- 11	Mean	ST Dev	CV	Min	Max
SiO_2	57.22	60.70	59.98	55.98	62.33	58.68	60.14	59.29	2.16	3.65	55.98	62.33
Al_2O_3	12.80	14.59	14.28	15.05	14.41	15.49	15.97	14.66	1.02	6.95	12.80	15.97
Fe_2O_3(T)	5.12	5.51	5.55	6.02	5.85	5.94	6.47	5.78	0.44	7.54	5.12	6.47
MnO	0.06	0.06	0.06	0.06	0.07	0.06	0.06	0.06	0.00	6.30	0.06	0.07
MgO	2.39	2.50	2.53	2.47	1.86	2.60	2.55	2.41	0.25	10.44	1.86	2.60
CaO	17.21	11.26	12.35	15.34	10.97	12.25	9.79	12.74	2.62	20.55	9.79	17.21
Na_2O	2.11	2.01	1.94	1.78	1.38	1.52	1.42	1.74	0.30	17.12	1.38	2.11
K_2O	2.11	2.37	2.33	2.28	2.13	2.43	2.51	2.31	0.15	6.43	2.11	2.51
TiO_2	0.74	0.81	0.81	0.82	0.83	0.86	0.90	0.82	0.05	5.77	0.74	0.90
P_2O_5	0.23	0.19	0.19	0.19	0.16	0.17	0.19	0.19	0.02	11.59	0.16	0.23
Element (ppm)	AG- 1	AG- 5	AG- 6	AG- 8	AG- 9	AG- 10	AG- 11	Mean	ST Dev	CV	Min	Max
Sc	10	11	11	11	11	12	12	11	1	6	10	12
Be	2	2	2	2	2	2	2	2	0	0	2	2
V	104	114	111	123	113	122	119	115	7	6	104	123
Ba	247	206	215	210	280	207	259	232	30	13	206	280
Sr	537	334	378	469	292	373	289	382	92	24	289	537
Y	19	21	21	20	22	22	22	21	1	5	19	22
Zr	229	201	213	190	247	197	185	209	22	11	185	247
Cr	80	90	90	90	90	90	90	89	4	4	80	90
Co	6	9	8	8	10	9	10	9	1	16	6	10
Ni	30	30	30	30	30	40	30	31	4	12	30	40
Cu	10	20	20	10	20	20	20	17	5	28	10	20
Zn	70	80	80	80	80	80	80	79	4	5	70	80
Ga	14	17	16	16	16	17	17	16	1	7	14	17
Ge	1	1	1	1	2	1	1	1	0	33	1	2
As	12	15	9	17	16	13	7	13	4	29	7	17
Rb	73	90	85	84	80	86	87	84	6	7	73	90
Nb	15	17	16	16	16	16	17	16	1	4	15	17
Mo	< 2	< 2	14	< 2	10	< 2	< 2	12	3	24	10	14
Ag	0.9	0.7	0.8	0.6	0.8	0.6	0.6	1	0	17	0.6	0.9
In	< 0.2	< 0.2	< 0.2	< 0.2	< 0.2	< 0.2	< 0.2					
Sn	2	2	2	2	2	2	2	2	0	0	2	2
Sb	< 0.5	< 0.5	< 0.5	< 0.5	0.5	< 0.5	< 0.5					
Cs	4	5	5	5	5	5	5	5	0	7	4	5
La	30	35	34	33	34	33	35	33	2	5	30	35
Ce	60	70	68	66	70	67	70	67	3	5	60	70
Pr	7	8	7	7	8	7	8	7	0	5	7	8
Nd	26	29	28	28	29	28	29	28	1	5	26	29
Sm	5	6	5	5	6	6	5	5	0	5	5	6
Eu	1	1	1	1	1	1	1	1	0	6	1	1
Gd	4	5	5	5	5	5	5	5	0	5	4	5
Tb	1	1	1	1	1	1	1	1	0	5	1	1
Dy	4	4	4	4	4	4	4	4	0	4	4	4
Ho	1	1	1	1	1	1	1	1	0	5	1	1
Er	2	2	2	2	2	2	2	2	0	4	2	2
Tm	0	0	0	0	0	0	0	0	0	5	0	0
Yb	2	2	2	2	2	2	2	2	0	5	2	2
Lu	0	0	0	0	0	0	0	0	0	4	0	0
Hf	6	6	6	5	7	5	5	6	1	10	5	7
Ta	1	1	1	1	1	1	1	1	0	7	1	1
W	1	1	1	1	1	1	1	1	0	0	1	1
Tl	0	0	0	0	0	0	0	0	0	13	0	0
Pb	16	18	19	16	18	16	18	17	1	7	16	19
Bi	< 0.4	< 0.4	< 0.4	< 0.4	< 0.4	< 0.4	< 0.4					
Th	8	10	9	9	10	9	9	9	0	4	8	10
U	3	3	3	3	2	3	3	3	0	10	2	3

geochemical markers, with an average value of 418 ppm and the highest CV, close to 47 %. It appears clear from examination of Table 5 that this anomalous CV is conditioned by the extraordinarily high concentration value (1115 ppm) measured in the sample M 179/324. Barium, as known, is an element that can be geochemically correlated to the content in minerals such as feldspar and carbonates, in which it is vicariant of the major elements like K and Ca. However, such a concentration can be considered as accidentally caused by the presence in the original clay paste of small quantities of evaporitic sulphates or by punctual contaminations that occurred in the burial phase. Even the Sr content, although to a lesser extent than Ba, is significantly higher than that found in local clays. To interpret this data, the same hypotheses illustrated for barium can be made. In contrast, for numerous other geochemically significant elements (i.e. V, Y, Zr, Cr, Co, Ni, Cu, Zn, As, Rb, Nb, La, Ce) it is possible to find a more than satisfactory matching with what was found in local clays and kiln wasters.

Overall, in the light of what emerged from the analyses, the chemical composition of the ceramic finds in this study is reasonably comparable with that of the clayey raw materials available a few hundred meters from the kilns site, and with that of the production wasters found in the same area. Therefore, it is plausible to consider the reference chemical composition of the amphoric productions of Agrigento, shown in Table 6, which represent the composition of raw materials, ceramic finds and production wasters.

6. Discussion

In antiquity, the setting-up of transport container manufacturing

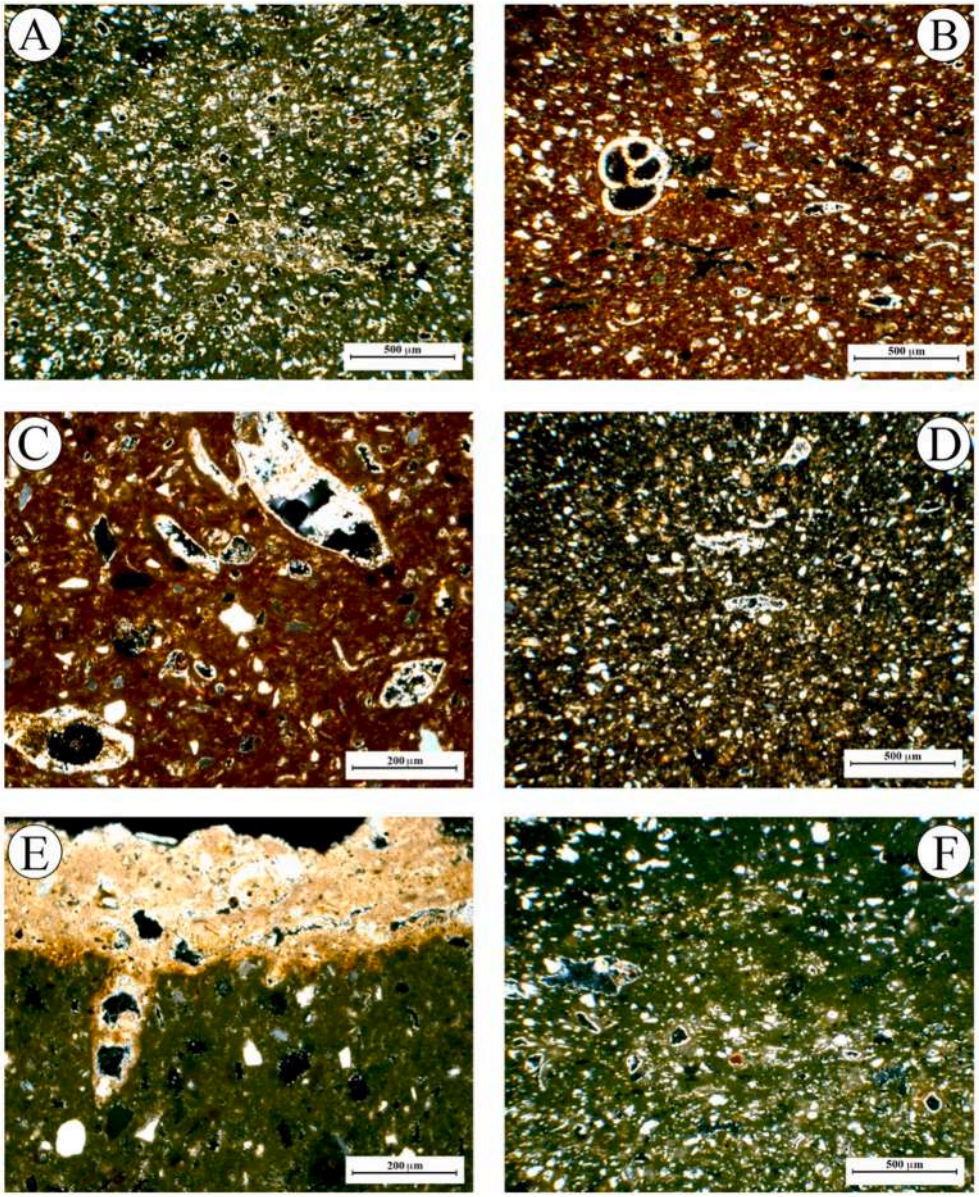

Fig. 13. Thin section microphotographs of some representative ceramic samples (XPL): (A-D) overview of the characterizing textural and compositional aspects; (B-C) recrystallized calcareous microfossils, micritic clots and pore casts; (E) presence of external deposits of secondary microcrystalline calcite; (F) textural and mineralogical aspects of the production waste.

installations implies the availability of an agricultural *surplus* destined for extra-local markets (Sourisseau, 2011). In the case of the western Greek amphorae here under discussion, the most probable commercial content is thought to be wine (Sacchetti, 2012 with earlier references). On-going research on the production of the present class in Sicily's Greek colonies has allowed for the identification, on the grounds of both archaeometric and archaeological analyses, of local series manufactured in Himera (Montana et al., 2020; Bechtold et al., 2019), Gela (Barone et al., 2012; Spagnolo, 2018), Selinunte (Bechtold, 2020c with references to on-going archaeometric research) and the in Strait of Messina-area (Barone et al., 2005; Barone et al., 2011; Spagnolo, 2002). As a result of socio-economic interaction on many levels, Greek-styled vessels imitating western Greek amphorae were also produced in the Punic *milieu* at Palermo and Solunto (Bechtold, 2020d with references to on-going archaeometric research) and in the native hinterland, in Entella and possibly in Monte Iato (Corretti et al., 2017; Corretti & Michelini, 2020). Based on the archaeological data currently available, the manufacture of the earliest type, Sourisseau's form 1α (Sourisseau, 2011) with *Randform* 1 (Gassner, 2003), is reliably documented only in northwestern Sicily, in the Dorian-Chalcidian colony of Himera which started to produce transport vessels during the third quarter of the 6th century BCE. About one generation later, towards the last quarter of the 6th century BCE, the dissemination of a veritable *koiné* of Greek-styled amphorae of Sourisseau's form 2 with *Randformen* 2–3 can be observed for large parts of Greek, Punic and indigenous western and southern Sicily (see above).

The present archaeometric research was aimed at verifying the compatibility of the local ceramic pastes with the clays of the *Narbone* Formation, cropping out in the whole area of the *Valle dei Templi* and even a few tens of meters from the furnace located close to the *Porta V*. The execution of firing tests on these clayey materials allowed to highlight with satisfactory detail the distinctive mineralogical-petrographic and chemical characteristics (markers) of the amphoric productions of Agrigento. These lower Pleistocene clays were considered particularly suitable for ceramic use, giving rise to a microfabric characterized by relatively fine aplastic inclusions with serial distribution, packing

Table 5
LOI normalized chemical composition of the ceramic fragments.

Element Oxide (wt%)	M179/ 232	M179/ 233	M179/ 324	M179/ 332	M208/ 1	M208/ 2	M208/ 3	M208/ 5	M209/ 1	M209/ 10	M209/ 3	M209/ 4	M209/ 5	M209/ 6	M210/ 1	M210/ 2	M119/ 174	Mean	Dev ST	CV	Min	Max	QAV_1	QAV_2
SiO_2	60.13	60.39	59.18	58.28	56.59	58.96	61.34	59.93	58.92	61.29	59.84	58.75	59.60	58.93	57.13	58.32	55.79	59.02	1.51	2.56	55.79	61.34	56.81	57.16
Al_2O_3	15.57	14.19	14.38	14.89	13.36	12.11	11.97	12.96	13.24	12.93	13.39	13.22	12.59	13.63	12.88	15.97	14.00	13.61	1.12	8.20	11.97	15.97	12.98	14.29
Fe_2O_3(T)	6.28	5.93	5.60	5.92	5.61	5.24	5.17	5.40	5.58	5.62	5.53	5.44	5.31	5.63	5.45	6.66	5.74	5.65	0.38	6.67	5.17	6.66	5.76	6.15
MnO	0.06	0.06	0.05	0.11	0.06	0.05	0.06	0.06	0.05	0.06	0.06	0.06	0.06	0.06	0.06	0.06	0.07	0.06	0.01	21.33	0.05	0.11	0.06	0.06
MgO	2.33	2.05	2.02	2.20	1.97	2.25	2.03	2.19	2.21	2.21	2.39	2.05	2.10	2.40	2.37	2.55	2.05	2.20	0.16	7.50	1.97	2.55	2.42	2.45
CaO	10.96	13.40	14.87	14.23	18.70	17.87	15.66	15.59	15.99	13.96	14.16	16.54	16.17	15.25	18.09	11.76	16.75	15.29	2.10	13.72	10.96	18.70	18.63	16.09
Na_2O	1.07	0.91	0.83	1.24	0.66	0.67	0.83	0.90	0.95	0.81	1.55	0.80	0.93	0.87	1.14	1.24	0.92	0.96	0.23	23.54	0.66	1.55	0.78	0.84
K_2O	2.50	2.05	2.07	2.18	2.00	1.90	1.92	1.97	2.02	2.12	2.08	2.13	2.17	2.13	1.88	2.32	2.16	2.09	0.16	7.46	1.88	2.50	2.03	2.24
TiO_2	0.90	0.84	0.81	0.76	0.77	0.71	0.72	0.76	0.78	0.77	0.79	0.76	0.74	0.76	0.75	0.89	0.77	0.78	0.05	6.74	0.71	0.90	0.74	0.84
P_2O_5	0.20	0.18	0.19	0.19	0.27	0.23	0.30	0.25	0.27	0.22	0.22	0.26	0.33	0.33	0.26	0.22	1.75	0.33	0.37	109.62	0.18	1.75	0.16	0.17
Element (ppm)	M179/ 232	M179/ 233	M179/ 324	M179/ 332	M208/ 1	M208/ 2	M208/ 3	M208/ 5	M209/ 1	M209/ 10	M209/ 3	M209/ 4	M209/ 5	M209/ 6	M210/ 1	M210/ 2	M119/ 174	Mean	Dev ST	CV	Min	Max	QAV_1	QAV_2
Sc	13	12	12	13	11	10	10	11	11	11	12	11	11	12	11	14	12	12	1	9	10	14	11	12
Be	2	2	2	2	2	2	2	2	2	2	2	2	2	2	2	2	2	2	0	0	2	2	2	2
V	113	113	113	94	92	85	96	96	104	97	111	101	88	97	95	127	106	102	11	11	85	127	108	123
Ba	328	296	1115	546	346	383	460	440	484	382	375	401	297	313	394	296	243	418	196	47	243	1115	308	614
Sr	402	590	670	463	626	708	577	738	657	599	628	579	508	605	773	404	741	604	111	18	402	773	1187	715
Y	26	24	23	23	23	22	22	23	23	23	25	22	22	23	22	25	24	23	1	5	22	26	26	24
Zr	217	272	256	185	234	253	274	267	261	264	304	250	249	226	267	211	159	244	36	15	159	304	322	328
Cr	100	90	100	100	90	70	80	90	90	80	80	90	80	80	80	110	80	88	10	12	70	110	90	100
Co	15	9	9	13	8	7	7	8	7	8	7	8	8	8	7	12	7	9	2	27	7	15	8	9
Ni	40	30	30	50	30	30	30	30	30	30	30	30	30	30	30	40	30	32	6	17	30	50	50	50
Cu	30	20	20	30	20	20	20	20	20	20	10	20	20	20	20	20	20	21	4	21	10	30	10	20
Zn	100	80	80	90	80	70	80	80	80	80	70	80	80	80	80	100	110	84	11	13	70	110	80	90
Ga	21	16	17	17	16	14	14	16	16	15	15	15	15	15	15	22	16	16	2	14	14	22	15	17
Ge	2	1	1	2	1	1	1	1	1	1	1	1	1	1	1	2	< 1	1	0	34	1	2	1	1
As	13	16	13	8	15	13	16	10	17	13	5	14	9	10	18	18	12	13	4	28	5	18	9	10
Rb	110	77	80	81	82	69	75	79	79	77	33	79	81	82	26	100	84	76	20	26	26	110	74	80
Nb	20	17	19	15	16	14	15	16	17	15	16	16	16	16	16	21	16	17	2	11	14	21	16	18
Mo	< 2	< 2	12	< 2	< 2	10	7	< 2	< 2	< 2	< 2	< 2	< 2	< 2	< 2	< 2	< 2	10	3	26	7	12	< 2	< 2
Ag	0.8	0.9	1	0.7	0.9	0.8	1	0.9	0.9	1	1	0.8	0.9	0.7	0.9	0.7	1.1	1	0	13	0.7	1.1	< 0.5	< 0.5
In	< 0.2	< 0.2	< 0.2	< 0.2	< 0.2	< 0.2	< 0.2	< 0.2	< 0.2	< 0.2	< 0.2	< 0.2	< 0.2	< 0.2	< 0.2	< 0.2	< 0.2						< 0.2	< 0.2
Sn	3	2	2	3	2	2	2	2	2	2	2	2	2	2	2	3	3	2	0	20	2	3	2	2
Sb	0.5	0.5	0.5	0.6	< 0.5	< 0.5	< 0.5	< 0.5	< 0.5	< 0.5	< 0.5	< 0.5	< 0.5	< 0.5	< 0.5	0.5	< 0.5	1	0	9	0.5	0.6	0.5	0.5
Cs	6	4	5	4	5	4	4	4	4	4	4	4	4	5	4	6	5	4	1	14	4	6	5	5
La	42	36	38	35	34	29	31	33	34	32	32	33	32	32	33	42	42	35	4	12	29	42	50	40
Ce	84	71	76	71	68	59	64	66	69	64	66	66	66	63	67	85	81	70	8	11	59	85	99	79
Pr	9	8	8	8	8	7	7	7	8	7	7	7	7	7	7	9	9	8	1	11	7	9	12	9
Nd	36	31	32	30	29	25	27	28	29	27	28	28	28	27	28	35	36	30	3	11	25	36	44	35
Sm	7	6	6	6	6	5	5	6	6	5	6	6	6	5	6	7	7	6	1	10	5	7	8	7
Eu	1	1	1	1	1	1	1	1	1	1	1	1	1	1	1	2	1	1	0	10	1	2	1	1
Gd	6	5	5	5	5	4	5	5	5	5	5	5	5	5	5	6	5	5	0	8	4	6	6	5
Tb	0.9	0.8	0.8	0.8	0.7	0.6	0.7	0.7	0.8	0.7	0.7	0.7	0.8	0.7	0.7	0.9	0.8	1	0	11	0.6	0.9	0.9	0.8
Dy	5	5	5	4	4	4	4	4	5	4	4	4	4	4	4	5	5	4	0	8	4	5	5	5
Ho	1	0.9	0.9	0.9	0.8	0.8	0.8	0.8	0.9	0.8	0.9	0.9	0.9	0.8	0.8	1	0.9	1	0	8	0.8	1	0.9	0.9
Er	3	3	3	3	3	2	2	2	3	2	3	3	3	2	2	3	3	3	0	8	2	3	3	3
Tm	0	0	0	0	0	0	0	0	0	0	0	0	0	0	0	0	0	0	0	6	0	0	0	0
Yb	3	3	3	3	2	2	2	2	3	2	3	2	2	2	2	3	3	2	0	7	2	3	3	3
Lu	0.4	0.4	0.4	0.4	0.4	0.3	0.4	0.4	0.4	0.4	0.4	0.4	0.4	0.4	0.4	0.4	0.4	0.4	0.0	7.7	0.3	0.4	0.4	0.4
Hf	6	7	7	5	6	6	7	7	7	6	8	7	7	6	7	6	5	6	1	12	5	8	7	7
Ta	2	1	1	1	1	1	1	1	1	1	1	1	1	1	1	2	1	1	0	11	1	2	1	1
W	2	5	2	2	1	1	1	1	1	1	< 1	1	1	< 1	< 1	1	1	2	1	73	1	5	< 1	1
Tl	0.4	0.3	< 0.1	0.3	0.2	0.2	0.2	< 0.1	0.1	0.1	< 0.1	< 0.1	< 0.1	< 0.1	< 0.1	< 0.1	0.2	0	0	44	0.1	0.4	< 0.1	< 0.1
Pb	23	19	15	21	24	17	20	16	20	36	6	19	19	20	14	14	19	19	6	32	6	36	11	11
Bi	< 0.4	< 0.4	< 0.4	< 0.4	< 0.4	< 0.4	< 0.4	< 0.4	< 0.4	< 0.4	< 0.4	< 0.4	< 0.4	< 0.4	< 0.4	< 0.4	< 0.4						< 0.4	< 0.4
Th	12	10	11	10	10	8	9	9	10	9	9	9	9	9	9	12	11	10	1	11	8	12	15	11
U	3	3	3	2	4	3	3	3	3	3	3	3	3	3	3	3	10	3	2	50	2	10	5	4

Table 6
Chemical reference group for Agrigento's ceramic productions.

Element Oxide (wt%)	Mean
SiO_2	59.05
Al_2O_3	14.13
Fe_2O_3(T)	5.73
MnO	0.06
MgO	2.32
CaO	14.12
Na_2O	1.34
K_2O	2.20
TiO_2	0.80
P_2O_5	0.25
Element (ppm)	Mean
Sc	11
Be	2
V	109
Ba	327
Sr	511
Y	22
Zr	231
Cr	88
Co	9
Ni	33
Cu	19
Zn	81
Ga	16
Ge	1
As	13
Rb	80
Nb	16
Mo	11
Ag	1
In	
Sn	2
Sb	1
Cs	5
La	35
Ce	69
Pr	8
Nd	29
Sm	6
Eu	1
Gd	5
Tb	1
Dy	4
Ho	1
Er	2
Tm	0
Yb	2
Lu	0
Hf	6
Ta	1
W	1
Tl	0
Pb	18
Bi	
Th	10
U	3

varying from 15 % to about 25 % (area), and silico-clastic component slightly prevalent or equivalent to the calcareous one.

Consequently, the present research has led to a detailed archaeometric and archaeological characterisation of Agrigento's late 6th-4th century BCE transport container series which has permitted, for the first time, to identify the distribution of wine (?) amphorae from *Akragas* in several consumption sites situated in Sicily and on Pantelleria. Therefore, this study contributes to the reconstruction of the economic activities of the city. Notably, among the steadily increasing group of late Archaic Sicilian towns producing western Greek amphorae, at present Agrigento stands out – as the only candidate – for a modest extra-local circulation of its transport container series (Fig. 2). A first case study is provided by the ample *corpus* (N = 556) of western Greek amphorae yielded by the necropoleis of Himera where vessels from Agrigento clearly outnumber other Sicilian series, exception made for the local amphorae (Bechtold, 2020b). However, the class seems well documented also in 5th-4th century BCE Pantelleria and in late Archaic Selinunte and Segesta, even if no quantitative assessment can be made yet.

The archaeometric and archaeological evidence obtained by our research is in perfect harmony with the ancient sources, which underline 5th-century BCE Agrigento's preeminent wine trade, specifically with Carthage's North African sphere of influence. To date, wine exports from *Akragas* seem particularly well attested during the late Archaic period, which corresponds to a period of general wide-spread health attested for southwestern and northwestern Sicily as a whole (Bechtold et al., 2019). Highly interestingly, the documentation in Himera of some early Classical-period amphorae originating from Agrigento might be related to the hegemonic phase under the reign of *Theron* and his son *Thrasydaios* (490/89–471 BCE) and the transitional decade until the democratic takeover in the Sicilian cities (461 BCE). These artefacts seem to represent archaeological markers of the expansion of Agrigento's political and economic sphere of influence over large parts of western Sicily along the South-North axis of the river valleys *Imera Meridionale/F. Salso* and *Imera Settentrionale* during the third and part of the fourth decade of the 5th century BCE (for a numismatic perspective, see: Leeck, 2020; an archaeological-historical analysis in: Caliò, 2019).

Amphorae data related to the second half of the 5th century BCE are still too scanty to allow for a wider interpretation of both local and extra-local circulation of the class under focus. Finally, and on the grounds of the current evidence, a new *floruit* of the consumption of wine grown at *Akragas* during the later 5th and the first half of the 4th century BCE is likely at least for Carthage's colony of *Cossyra*.

7. Conclusions and perspectives for further research

The interdisciplinary, archaeological and archaeometric method implemented in the present research is highly encouraging in view of further investigation of new amphorae materials, which should especially shed light on the span of time comprised between the Emmenidian tyranny (490/89–471 BCE) and the later 5th century BCE, currently almost absent in our archaeological record. The issue is particularly intriguing as this period represents a moment of crisis for central western Sicily, characterised by the abandonment or at least the restriction of many native sites situated in the *hinterland* of the colonies (Vassallo, 2020; Kistler, 2020; Michelini, 2021). Recently, this archaeological phenomenon, accompanied by a reduction of the local coinage strongly shaped by the motives of the series of *Akragas*, has been linked to the decrease of the Emmenidian political and economic influence over large parts of western Sicily (Leeck, 2020). Put into perspective, fabric studies on western Greek amphorae from archaeological deposits dating to the second third of the 5th century BCE could answer the question if Agrigento's loss of influence can be observed within the amphorae record.

Funding

This research was funded by the Austrian Science Fund (FWF): P 30030-G25, in the frame of the project "Trade of western Greek amphorae (6th-5th century BCE) from the perspective of Himera (western Sicily): a contribution to the identification of production centres, typological repertoires and distribution patterns". Open Access Funding by the Austrian Science Fund (FWF).

CRediT authorship contribution statement

G. Montana: Conceptualization, Investigation, Supervision, Visualization, Resources, Writing – original draft, Writing – review & editing. **L. Randazzo:** Conceptualization, Investigation, Supervision, Visualization, Resources, Writing – original draft, Writing – review & editing. **M.**

Gasparo Morticelli: Investigation, Visualization, Writing – original draft. **V. Baldoni:** Investigation, Visualization, Writing – original draft. **B. Bechtold:** Conceptualization, Investigation, Supervision, Visualization, Resources, Funding acquisition, Writing – original draft, Writing – review & editing.

Declaration of Competing Interest

The authors declare that they have no known competing financial interests or personal relationships that could have appeared to influence the work reported in this paper.

Data availability

No data was used for the research described in the article.

Acknowledgments

M. de Cesare, C.E. Portale and A. Amico (Università degli Studi di Palermo) are acknowledged for the kind permission to include 19 pottery samples yielded by the excavations in the area south of the temple of Zeus in Agrigento (Section 2.2) in the present archaeometric research. The Parco Archeologico e Paesaggistico della Valle dei Templi di Agrigento is acknowledged for the kind permission to collect samples of clayey raw materials. Thanks to R. Lampl (Universität Wien) for the composition of Fig. 3 and F. Ferlito (Università di Catania) for the setting up of Figs. 1-2, 4-6. Figs. 8-9 were set up by M. Gasparo Morticelli, while Figs. 10-13 by G. Montana. and L. Randazzo.

Thanks to Campbell Orchard, Department of Classics and Ancient History, University of Warwick, for proofreading the article. Finally, the authors are indebted to two anonymous reviewers for their critical comments on the manuscript.

Appendix A. Supplementary material

Supplementary data to this article can be found online at https://doi.org/10.1016/j.jasrep.2022.103627.

References

Alaimo, R., Di Franco, L., Giarrusso, R., Montana, G., 1995. Appendice II: Analisi mineralogiche e petrografiche. Descrizione mineralogico-petrografica dei prodotti ceramici. In: Bonacasa Carra (ed.), Agrigento. La necropoli paleocristiana subdivo, Roma, 372-415.

Amico, A., 2020. Anfore greco-occidentali dall'area a Sud del Tempio di Zeus ad Agrigento: una selezione. In: FACEM (version December/06/2020). (Accessed 12 September 2022).

Baldoni, V., Scalici, M., 2020. Un'officina per la produzione ceramica ad Agrigento: prime anticipazioni sui dati di scavo e analisi dei materiali dal Quartiere fuori Porta V (QAV). In: FACEM (version December/06/2020) (http://www.facem.at/project-papers.php).

Baldoni, V., Parello, M.C., Scalici, M., 2019. New researches on Pottery workshops in Akragas. Excavations in the artisanal area outside Gate 5 (excavation 2019). Ocnus 27, 107–116.

Barone, G., Branca, C., Crupi, V., Ioppolo, S., Majolino, D., Puglisi, G., Spagnolo, G., Tigano, G., 2003. Archaeometric analyses on ceramics from Sicilian Greek oclonies: a contribution to the knowledge of Messina, Gela and Agrigento production. Per. Mineral 73, 43–56.

Barone, G., Crupi, V., Galli, S., Majolino, D., Migliardo, P., Spagnolo, G., 2004. Mineralogical-petrographic and spectroscopic ionvestigations on coarse pottery and transport amphorae from Agrigento. Mediterranean Archaeol. Archaeometry 4 (1), 47–59.

Barone, G., Ioppolo, S., Majolino, D., Branca, C., Sannino, L., Spagnolo, G., Tigano, G., 2005. Archaeometric analysies on pottery from archaeological excavations in Messina (Sicily, Italy) from the Greek archaic to the Medieval age. Per. Mineral 74 (1), 11–41.

Barone, G., Belfiore, C.M., Mazzoleni, P., Spagnolo, G., Tigano, G., Triscari, M., 2011. Le anfore commerciali dell'Occidente greco in età arcaica e classica: problemi di localizzazione delle fabbriche. In: Gualtieri, S., Starnini, E., Cabella, R., Capelli, C., Fabbri, B. (Eds.), La ceramica e il mare, Atti della XII Giornata di Archeometria della Ceramic (Genova 2008), Roma, 87-102.

Barone, G., Mazzoleni, P., Spagnolo, G., Aquilia, E., 2012. The transport amphorae of Gela: a multidisciplinary study on provenance and technological aspects. J Archaeol. Sci 39 (1), 11–22. https://doi.org/10.1016/j.jas.2011.06.018.

Bechtold, B., Vassallo, S., Ferlito, F., 2019. La produzione delle anfore greco-occidentali di Himera: uno studio sulla loro identificazione. Notiziario Archeologico della Soprintendenza di Palermo 51 (2019).

Bechtold, B., 2020a. First observations on western Greek amphorae produced at Akragas. In: FACEM (version December/06/2020) (http://www.facem.at/project-papers.php).

Bechtold, B., 2020b. Prime osservazioni sulla produzione di anfore greco-occidnetali in alcune città della Sicilia: il contributo degli scavi di Himera. In: M. Chiovaro/R. Sapia (eds.), Studi in onore di Stefano Vassallo. Regione Siciliana. Assessorato dei Beni Culturali e dell'identità siciliana, Palermo, 134-142, http://www.regione.sicilia.it/beniculturali/dirbenicult/NotiziarioArcheoPalermo.html.

Bechtold, B., 2020c. First evidences for western Greek amphorae produced at Selinus. In: FACEM (version December/06/2020) (http://www.facem.at/project-papers.php).

Bechtold, B., 2020d. Western Greek amphorae produced at Panormos and/or Solus. In: FACEM (version December/06/2020) (http://www.facem.at/project-papers.php).

Bigi, G., Decima, A., Bommarito, S., La Rosa, N., Aiello, R. 1972. Carta geologica d'Italia alla scala 1:50.000 del foglio 636 Agrigento. ISPRA, Servizio Geologico d'Italia. Grafica editoriale cartografica. Roma.

Brun, J.-P., 2011. La produzione del vino in Magna Grecia e in Sicilia. In: La vigna di Dioniso: vite, vino e culti in Magna Grecia. Atti del quarantanovesimo convegno di Studi sulla Magna Grecia (Taranto 24-28 settembre 2009), 97-142. Taranto.

Caliò, L., 2019. Agrigento e il teatro nell'urbanistica della città. Storia di un centro monumentale. In: Caliò, L., Lepore, G. (Eds.), Agrigento: Archaeology of an ancient city. Urban form, sacred and civil spaces, productions, territory, Panel 8.2. In: Bentz, M., Heinzelmann, M.(eds.), Proceedings of the 19th International Congress of Classical Archaeology (Cologne/Bonn, 22 – 26 May 2018), Archaeology and Economy in the Ancient World, Heidelberg, 37-62.

Caliò, L.M., Gerogiannis, G.M., Giannella, F., Livadiotti, M., Fino, A., Albertocchi, M., Leoni, F., 2016. Il santuario ellenistico romano di Agrigento. Lo scavo, l'inquadramento urbano, l'architettura. In: Parrello, M.C., Rizzo, M.S. (Eds.), Paesaggi urbani tardoantichi. Casi a confronto. Atti delle Giornate Gregoriane VIII Edizione (29-30 novembre 2014), Bari, 295–318.

Catalano, R., Valenti, V., Albanese, C., Accaino, F., Sulli, A., Tinivella, U., Gasparo Morticelli, M., Zanolla, C., Giustiniani, M., 2013. Sicily's fold/thrust belt and slab rollback: the SI.RI.PRO. seismic crustal transect. – J. Geol. Soc. London 170, 451–464.

Cau Ontiveros, M.A., Day, P.M., Montana, G., 2002. Secondary calcite in archaeological ceramics: evaluation of alteration and contamination processes by thin section study, In: V. Keklikoglou, A. Hein, Y. Maniatis (Eds.), Proceedings of the 5th European Meeting on Ancient Ceramics (Athens, 18-20 October 1999), Modern Trends In Scientific Studies on Ancient Ceramics. British Archaeological Reports (BAR), International Series 1011 Archaeopress Oxford, UK, pp. 9–18.

Corretti, A., Michelini, C., 2020. Entella (Contessa Entellina, PA). Produzioni locali e importazioni di anfore nella città e nel territorio (VI-inizio III sec. a.C.). In: FACEM (version Decembre/06/2020) (http://www.facem.at/project-papers.php).

Corretti, A., Michelini, C., Montana, G., Randazzo, L., 2017. Entella. Nuove attestazioni di produzioni ceramiche: vasi decorati a stampo e anfore commerciali. AnnPisa 9 (2 suppl.), 67–85.

Cotecchia, V., Fiorillo, F., Monterisi, L., Pagliarulo, R., 2005. Slope Instability in the Valley of Temples, Agrigento (Sicily). Giornale di Geologia Applicata 1, 91–101.

De Bonis, A., Gassner, V., Ntaflos, T., Rizzo, M.L., Sauer, R., Serritella, A., Vassallo, S., Bechtold, B., 2020. 5th-century BC Himera and the Campanian Connection: Petrographic and Archaeological Studies on Western Greek Amphorae from Poseidonia and Elea Unearthed in the Necropolis of Himera. Minerals 10 (3), 227.

de Cesare, M., Portale, C.E., 2017. Le ricerche dell'Università di Palermo nel santuario di Zeus Olympios ad Agrigento. In: Sojc, N. (Ed.), Akragas: Current Issues in the Archaeology of a Sicilian Polis, Leiden, 91-94.

de Cesare, M., Bechtold, B., Cipolla, P., Quartararo, M., 2020. Segesta e il mondo greco attraverso lo studio delle anfore greco-occidentali da santuari: primi dati. Thiasos 9 (1), 349–378.

FACEM: Gassner, V., Trapichler, M., Bechtold, B. (eds.), Provenance Studies on Pottery in the Southern Central Mediterranean from the 6th to the 2nd c. B.C. In: FACEM (version 06/12/2020) (http://www.facem.at/project-papers.php).

Ferlito, F., 2020. Fabrics of Akgragas. In: FACEM (version December/06/2020) (http://www.facem.at/project-papers.php).

Gassner, V., 2003. Materielle Kultur und kulturelle Identität in Elea in spätarchaisch-frühklassischer Zeit. Untersuchungen zur Gefäß- und Baukeramik aus der Unterstadt (Grabungen 1987-1994). Archäologische Forschungen 8. Velia-Studien 2, Wien.

Gassner, V., 2015. Le anfore greco-occidentali: riconsiderando la loro evoluzione e l'identificazione dei centri di produzioni. In: Poure, R. (Ed.), Contacts et acculturations en Méditerranée occidentale. Hommage à Michel Bats (Hyères 2011), Études Massaliètes 12, Aix-en-Provence, 345-356.

Hans, L.M., 1983. Karthago und Sizilien: die Entstehung und Gestaltung der Epikratie auf dem Hintergrund der Beziehungen der Karthager zu den Griechen und den nichtgriechischen Völkern Siziliens (VI.–III. Jahrhundert v. Chr.), Hildesheim.

Kistler, E., 2020. The Late Archaic House at Monte Iato: Greek-Style Architecture, Ritual Abandonment and the Politics of Indigeneity in Western Sicily (500–460/50 BC). Ancient West and East 19, 43–78.

Klug, R., 2020. Provenienzanalysen an den griechischen Amphoren. In: Bergemann, J. (Ed.), Der Agrigent-Hinterland-Survey. 3000 Jahre Siedlungsgeschichte in den Monte Sicani, Rahden/Westf., 64-66.

Leeck, Ch., 2020. Die frühe Tyrannis und der Raum. Die Münze als Quelle für die politische Funktionalisierung des Raumes unter der Emmenidenherrschaft in Akragas, Westsizilien (490/89-471 v. Chr.), Marburger Beiträge zur Antiken Handels-, Wirtschafts- und Sozialgeschichte 37 [2019], 1-52.

Marconi, C., 2014. Nuovi dati sui culti del settore meridionale del grande santuario urbano di Selinunte. Sicilia Antiqua 10, 263–271.
Marconi, C., Micchichè, R., Ward, A., 2017. Contextualizing an Animal Sacrifice in the Foundation of Temple R. A Preliminary Report of the Institute of Fine Arts – NYU Excavations on the Acropolis of Selinunte (2013–2015 Campaigns). Mare Internum. Archeologia e culture del Mediterraneo 9.
Matthew, A.J., Woods, A.J., Oliver, C., 1991, Spot Before The Eyes: New Comparison Charts for Visual Percentage Estimation in Archaeological Material, in Recent Developments in Ceramic Petrology. In: Middleton, A., Freestone, I. (Eds.), 211-263, British Museum Occasional Paper 81, London.
Michelini, C., 2021. L'età tardo-classica ed ellenistica: dai Campani di Entella a Sesto Pompei. In: Corretti, A., Gulletta, M.I., Michelini, C., Vaggioli, M.A. (Eds.), Entella II. Carta archeologica del Comune di Contessa Entellina dalla preistoria al medioevo, Pisa, v. III, 35-110.
Montana, G., 2011. Le argille ceramiche della Sicilia occidentale e centrale (Terra e ambiente 2). IlionBooks, Enna.
Montana, G., 2020. Ceramic raw materials: how to recognize them and locate the supply basins—mineralogy, petrography. Archaeol. Anthropol. Sci. 12 (8), 175.
Montana, G., Heinzel, C.E., Polito, A.M., Randazzo, L., 2012. Archaeometric evidence attesting production of indigenous archaic pottery at Monte Polizzo (Western Sicily). Periodico di Mineralogia 81 (1), 107–130. https://doi.org/10.2451/2012PM0007.
Montana, G., Randazzo, L., Bechtold, B., 2020. The Beginning of Western Greek amphorae Production in Western Sicily: archaeometric and Archaeological Studies on 6th-5th Centuries BCE Amphorae Manufactured in Himera. Minerals 10, 762.
Sacchetti, F., 2012. Les amphores grecques dans le Nord de l'Italie. Échanges commerciaux entre les Appennins et les Alpes aux époques archaïque et classique. Bibliothèque d'Archéologie Méditerranéenne et Africaine 10, Aix-en Provence.
Scalici, M., 2019. Produzione agricola e luoghi di trasformazione ad Agrigento. In: Dialoghi sull'Archeologia della Magna Grecia e del Mediterraneo. Atti del III Convegno Internazionale di Studi (Paestum 2018), III.4, 769-80. Napoli.
Schäfer, Th., Schmidt, K., Osanna, M. (Eds.), 2015. Cossyra I. Ergebnisse der Grabungen auf der Akropolis von S. Teresa/Pantelleria. Der Sakralbereich (Tübinger Archäologische Forschungen 10), Rahden/Westf.
Schreiber, B.C., Friedman, G.M., Decima, A., Schreiber, E., 1976. Depositional environments of Upper Miocene (Messinian) evaporite deposits of the Sicilian Basin. Sedimentology 23 (6), 729–760.
Sourisseau, J.-Ch., 2011. La diffusion des vins grecs d'Occident du VIIIe au IVe s. av. J.-C., sources écrites et documents archéologiques. In: La vigna di Dioniso: vite, vino e culti in Magna Grecia, Atti del 49 Convegno di Studi sulla Magna Grecia (Taranto 2009), 145-252.
Spagnolo, G., 2002. Anfore da trasporto arcaiche e classiche nell'occidente greco: nuove acquisizioni da recenti rinvenimenti a Messina. In Bacci, G.M., Tigano, G. (eds.), da Zancle a Messina un percorso archeologico attraverso gli scavi. II**, Messina, 31-46.
Spagnolo, G., 2018. La produzione di anfore da trasporto a Gela. In: Bernabò Brea, M., Cultraro, M., Gras, M., Martinelli, M.C., Pouzadoux, C., Spigo, U. (Eds.), A Madeleine Cavalier, Naples, 281-294.
van Der Mersch, C., 1996. Vigne, vin et économie dans l'Italie du Sud grecque à l'époque archaïque. Ostraka 1, 155–187.
Vassallo, S., 2005. Himera. Città greca. Guida alla storia e ai monumenti. Palermo.
Vassallo, S., 2018. Bibliografia ragionata sulle necropoli di Himera. In: Notiziario Archeologico Soprintendenza Palermo 30 https://www.regione.sicilia.it/beniculturali/dirbenicult/NotiziarioArcheoPalermo.html.
Vassallo, S., 2020. Guerre e conflitti nella Sicilia centro-occidentale tra la metà del VI e la fine del V sec a.C.: una prospettiva archeolologica. In: Jonasch, J. (Ed.), The fight for Greek Sicily. Society, Politics, and Landscapes, Oxford, 1-17.